# MASW for Shear Wave Velocity Evaluation of Soil Before and After Deep Dynamic Compaction Operations

by

Choon B. Park and Richard D. Miller

Kansas Geological Survey
University of Kansas
1930 Constant Avenue, Campus West
Lawrence, Kansas 66047-3726
Tel: 785-864-2162  Fax: 785-864-5317
Emails: park@kgs.ku.edu, rmiller@kgs.ku.edu

**KGS Project Number: IN34290**

December 8, 2003

**KGS Open-File Report 2003-64**

## ABSTRACT

Two surveys of multichannel analysis of surface waves (MASW) method were conducted over a soil site in Tacoma Water's Green River Facility, Washington, where a chemical treatment facility had been planned. Purpose of the surveys was to compare soil stiffness characterized by shear-velocity (Vs) distribution before and after Deep Dynamic Compaction (DDC) operations that were designed to improve the soil stiffness. Site soil consisted of very heterogeneous gravel and cobbles in a sand-and-silt matrix. Results from each survey are represented by two 2-D Vs maps delineating Vs variation of soil below the surveyed lines. One map was constructed from those dispersion curves that were analyzed with significant amount of subjective judgment involved, whereas the other map was constructed from those dispersion curves analyzed with as much objective information as possible. Comparison of 2-D Vs maps indicates that Vs actually reduced after the DDC operations, possibly due to the loss (or reduction) of cohesive bonding between soil particles caused by the compaction operations.

## INTRODUCTION

Soil stiffness is one of the critical parameters considered during an early stage of most geotechnical construction. It is related directly to the stability of structural foundation, especially under possible earthquake hazard. Soil of insufficient stiffness may go through a significant reduction of strength under earthquake shaking and liquefaction can occur that is responsible for tremendous amounts of damage in historical earthquakes around the world (Richart et al., 1970). A minimal soil stiffness is therefore strictly enforced for construction of buildings at earthquake-prone areas. This is especially the case if damage of the building may cause a significant threat to public safety as with a chemical treatment facility.

Traditionally, several geotechnical or geophysical methods have been used; for example, cone penetration test (CPT) (Lunne, 1997) and down-hole seismic (Dobrin and Savit, 1988) methods. CPT is an in-situ method that evaluates the stiffness by measuring resistance to penetrating probe. On the other hand, down-hole method is a seismic method that measures seismic velocities that are linked to the stiffness. Shear wave velocity (Vs) is the best indicator of the stiffness among all other elastic parameters of materials (Bullen, 1963). CPT and down-hole methods require drilling holes for insertion of the probes and they would give stiffness information only within a localized volume around the hole. Shear-wave down-hole method is generally known to be difficult because of difficulties in generating pure shear waves and also difficulties in processing acquired data.

Recently, surface waves are more often used to deduce the Vs structure of soil because of a greater effectiveness in data acquisition and processing (Miller et al., 1999; Stokoe et al., 1994). Propagation velocity (called phase velocity) of surface waves are frequency (or wavelength) dependent (this property is called dispersion). This dependency is determined mainly by the vertical Vs variation of soil. By recording surface waves of the fundamental-mode Rayleigh type propagating horizontally and

directly from the seismic source, the dispersion property is measured and usually represented by a curve (called dispersion curve) depicting variation of phase velocities with frequency. This curve is then used to back-calculate the vertical variation of Vs (called 1-D Vs profile) through a process called inversion. Although generally known to be a relatively easy seismic method, several complications may interfere with effectiveness of the surface-wave method if not properly handled by acquisition or processing (or both) techniques. Strong higher modes of surface waves and body waves of direct arrivals can often disturb the procedure to assess the fundamental-mode dispersion curve. In some cases where Vs changes rapidly with depth, generated surface waves may contain a significant amount of leaky modes whose energy dissipates rapidly into medium so that no fundamental mode of appreciable energy is recorded. In these cases, unstabilized and unpredictable propagation characteristics of the leaky modes may be misinterpreted as normal modes of surface waves if not detected accordingly.

The multichannel analysis of surface waves (MASW) method (Park et al., 1999a; Xia et al., 1999; Miller et al., 1999) utilizes some of the pattern-recognition concepts provided by the multichannel recording and processing approaches. It employs multiple receivers (geophones) placed along a linear survey line with an equal spacing, and seismic waves generated by an impulsive source (like a sledgehammer) and propagating along the receiver line are recorded synchronously, enabling the recognition of various types of propagation characteristics (Figure 1). Similar ability of pattern recognition provided by multichannel recording has long been utilized in the seismic exploration for natural resources (Telford et al., 1976). The main feature of seismic pattern recognized by the MASW is the frequency dependency of phase velocities (dispersion property) for all types of seismic waves propagating horizontally. In fact, dispersion property is first imaged (rather than calculated) by an objective wavefield transformation method that delineates the property from accumulation of energy detected by a proper pattern-recognition technique (Park et al., 1998) (Figure 2). The necessary dispersion of the fundamental mode Rayleigh waves is then identified in the image and a corresponding signal curve is extracted to be used for the next inversion step. A 1-D Vs profile is obtained from the inversion and this profile best represents the vertical Vs structure at the middle of the receiver spread used for the analysis. Because of this enhanced effectiveness in data processing, one measurement with one impact and one source-receiver (SR) configuration is usually enough to produce a 1-D Vs profile. By subsequently moving the same SR configuration along a preset survey line, multiple measurements can be made efficiently to produce multiple number of 1-D Vs profiles that are used to construct a 2-D Vs map (Figure 3). This 2-D Vs map represents a cross-sectional view of Vs distribution below the survey line.

Construction of a chemical treatment facility had been planned at Tacoma Water's Green River facility (Figure 4). Based on shear wave velocities (Vs's) below 500 ft/sec evaluated from a previous survey during the design phase in October 2002, soil improvements had been planned to reach minimal Vs of 850 ft/sec or higher for the uppermost 20 ft of soil. With a very heterogeneous soil consisting of gravel and cobbles in a sand-and-silt matrix, Deep Dynamic Compaction (DDC) was planned to be applied. DCC operations involve the dropping a 5 to 30 ton weight from heights of 30 to 120 ft

and are intended to sufficiently improve the Vs property of soil at the site. Two MASW surveys were performed before and after the DDC operations. Purpose of the surveys was to assess any improvement in Vs of soil resulting from the DDC operations. The pre-compaction survey was performed on September 10 and the post-compaction survey on November 5, 2003. Maximum depth of investigation was chosen to be at or near 25 ft.

## GENERAL PROCEDURE WITH MASW METHOD

Multiple number of receivers are deployed along a linear survey line with an equal spacing (receiver spacing) (Figure 1). Usually low-frequency (4.5 Hz) geophones are used as receivers and a heavy impact seismic source like a 10-lb sledgehammer is used. Distance ($x_1$) between source and the nearest-receiver-station (called source offset) is chosen in such a way that the near-field effects caused by excessive stress-strain relationship from the impact source are minimized (Park et al., 2002; 2001). This source offset is usually chosen to be about the same as maximum depth of investigation. However, it can be a certain fraction of it (Park et al., 1999a). The receiver spacing ($dx$) is chosen in such a way that it avoids any possible spatial aliasing for the shortest wavelength investigated and maximize the effectiveness of dispersion analysis (Park et al., 2001). Total length of receiver spread ($x_T$) (therefore, the farthest offset) needs to be short enough so that the strong body and higher-mode surface waves usually dominating at far offsets do not adversely affect the analysis of the fundamental-mode dispersion curve. Once source offset, receiver spacing, and the farthest offset are selected, this determines a specific source-receiver (SR) configuration. One measurement consists of a multichannel record (called a shot gather) acquired from one seismic impact (or sometimes from stacking records of multiple impacts together) in which vertical vibration history of surface at each geophone is represented by a time series called trace (Figure 1). In a survey to generate a 2-D Vs map, a chosen SR configuration is consistently moved by the same distance (called source interval) along the survey line until it covers most of distance to be surveyed. This type of data acquisition is called a roll-along mode (Sheriff and Gedart, 1982).

General scheme of data processing consists of following steps:

1. discarding noise shot gathers;
2. converting raw seismic data (SEG-2 format) into KGS format by combing all shot gathers to be processed;
3. encoding field geometry into the KGS-converted data and recompiling into the roll-along mode data set;
4. viewing all shot gathers to assess general signal-to-noise (S/N) ratio;
5. select several shot gathers at the beginning, in the middle, and at the end of survey line and process them for dispersion images to determine optimum ranges for frequency and phase velocity;
6. dispersion-curve analysis for all the shot gathers;
7. inversion analysis for all the dispersion curves analyzed; and

8. constructing 2-D Vs map from the inversion results by using an appropriate 2-D interpolation scheme.

Shot gathers with false triggering or with too-low S/N are discarded in step 1 and all remaining ones are converted into KGS format to be combined into a single file of increasing field file number (record number) in step 2. In step 3, station numbers for source and receivers and the receiver spacing are encoded into each record in the combined file. Then, all the encoded records are recompiled into the equivalent roll-along mode data set by discarding certain portions of traces in each record. All the records are then viewed for a general assessment of data quality (S/N) in step 4. Then, in step 5 are examined several records obtained from several different locations on the survey line on their dispersion characteristics by using the imaging method (Park et al., 1998). During this step, optimum range of frequency and phase velocity are chosen and they are used consistently for all the records to be processed. Each record is then processed to generate a dispersion image (called overtone image) in which the fundamental-mode dispersion trend is identified and a signal dispersion-curve is extracted based on the identified image in step 6. Once all the necessary dispersion curves have been extracted, then they will be exported to next processing stage of inversion in step 7. During this step, one 1-D Vs profile is obtained from each dispersion curve imported that represents Vs variation with depth at the middle of the receiver spread. When all 1-D Vs profiles are obtained for all dispersion curves, a proper 2-D interpolation scheme (for example, bilinear or Kriging scheme) is used to construct the final 2-D Vs map in step 8.

## DATA ACQUISITION

The pre-compaction survey was performed on September 10 and the post-compaction survey on November 5, 2003. Approximate locations of both survey lines are indicated in one of the site photos taken and a schematic of the lines is displayed in Figure 4. Post-compaction line was chosen slightly different from the pre-compaction line after its appropriateness was reassessed.

### Pre-Compaction Survey (Line 2000)

A receiver spacing (*dx*) (therefore station spacing) of 2 ft was chosen to account for possibly extremely low (usually lower than 200 ft/sec) Vs in the soil. Source offset ($x_1$) of 12 ft (6 *dx*) was chosen to account for the near-field effects. A source interval of 4 ft (2 *dx*) was chosen by considering possible degree of horizontal heterogeneity of Vs in the area. One complete receiver spread consisted of 72 (4.5 Hz) geophones connected by three 24-takeout cables. Three of 24-channel seismograph (Geometrics Geode) were connected to each cable and all three were configured to become one 72-channel acquisition system by combining them through Ethernet connections. A 16-lb sledgehammer was used as seismic source and each shot gather was obtained from one vertical impact of this hammer. A small rectangular (6 inch by 6 inch) metal plate was used as a baseplate upon which impact was applied. Purpose of using 72-channel system was to simulate the conventional roll-along mode acquisition with an additional advantage of diversity in data manipulation. The first shot location was at station 1999

with first geophone planted at station 2005 so that the chosen source offset (6 *dx*) could be maintained from the very first shot gather. Then, the source location moved by two stations (2 *dx*) into higher-number stations and the entire 72-receiver spread was left stationary until the source was moved by 48 times. This mode of source increment with the given SR configuration allows simulation of 24-channel roll-along acquisition mode by recompiling traces in each 72-channel record during the early stage of data processing (step 3). After 48 shots were delivered, then the first 48 receivers were moved after the end of the receiver spread and seismographs were reconfigured to make the 72-channel system. Stations were flagged from 2000 to 2315 and this station range represents those surface points where seismic data were recorded at least once. Shot points started from station 1999 and continued to station 2289 with a two-station interval. Sampling interval of 0.5 ms was used with total recording time of 1000 ms. Each shot was recorded with a single impact without any vertical stacking. No acquisition filters were used.

Ground condition was extremely soft and rough for approximately the front half of the survey line and baseplate was stuck into soil by as much as half to one foot at each impact. This part of the survey line resulted in those shot gathers in which dispersion characteristics are complicated and usually lacked coherency as discussed in the section of dispersion-curve extraction. Ground condition became less soft and the surface got less rough for the second half of the survey line.

All the shot gathers collected are displayed in Appendix I. Each shot gather is displayed in its first 500-ms portion and its relative location of receiver spread within the entire flagged survey line is indicated in a rectangular inset.

**Post-Compaction Survey (Line 4000)**

Survey line was chosen slightly different from the previous pre-compaction line after reassessment of the relative significance in Vs evaluation within the site was made. Basically the same source-receiver configuration and recording parameters were used as in the pre-compaction survey. However, the source increment was chosen to be a 4-station interval (8 ft) instead of 2-station interval. This was determined based on the horizontal heterogeneity of soil evaluated from the pre-compaction data. Stations were flagged from 4001 to 4250. Source station was moved from 3996 to 4239.

Ground condition was extremely soft and rough for most of the survey line. Although it gradually became less soft and less rough as approaching the second half of the line, the condition in general was softer and more rough than in the pre-compaction survey, possibly due to the disturbance caused by the compaction operations. Although top portion of the ground was slightly frozen during the early stage of the survey, it melted and became very muddy in the middle of the day as the acquisition got closer to the second half of the line.

All the shot gathers collected are displayed in Appendix II. Each shot gather is displayed in its first 500-ms portion and its relative location of receiver spread within the entire flagged survey line is indicated in a rectangular inset.

## DATA PROCESSING — DISPERSION ANALYSIS

Several shot gathers were chosen that were acquired at front, middle, and end portions of the survey line and they were used for preliminary processing to assess optimum ranges of frequency and phase velocity to be used during the overtone analysis. By using the assessed ranges, then each shot gather was transformed into the overtone image by the 2-D wavefield transformation method. It was then attempted to identify the fundamental-mode dispersion trend from which the signal dispersion-curve was extracted if properly identified. All this procedure with dispersion analysis was accomplished by using the surface-wave processing software (SurfSeis v. 1.5, 2003) developed at the Kansas Geological Survey. More details of the dispersion-curve extraction are explained in the following for both surveys.

### Pre-Compaction Analysis

Overtone images of all shot gathers collected are displayed in Appendix III. Images obtained from those shot gathers (records approximately in 2001-2030) collected at about first one third of the line indicate so complicated energy trend that any coherent energy trend that could be identified as the fundamental-mode surface waves is hardly recognized. This is believed due to the extremely soft condition at the ground surface and/or in the soil that either prevented the generation of stabilized surface waves or imparted most of seismic energy into the form of leaky modes of surface waves and normal compressional body waves. Coherent trend of energy is identified for the subsequent records in an approximate range of 2034 - 2045. This trend occurs in the frequency range of 20-50 Hz with a phase-velocity range of 250-1250 ft/sec. Then, the trend starts to break up in the subsequent records of 2046-2061 approximately. Then, another coherent trend starts to appear only with a significantly different phase velocity range (200-500 ft/sec). This changing pattern of the trend from coherent to broken and then back to coherent indicates that there is a significant seismic velocity (Vs) change along the horizontal direction between the two coherent zones. Although there are intermittent breaks in this trend of low phase velocities for the rest of the images, the general low-velocity trend of dispersion is maintained throughout the rest of the images (records of 2062-2155).

Using SurfSeis (2003), it was attempted to extract one fundamental-mode dispersion curve from each shot gather after examination of the corresponding overtone image. First, a reference point was assigned on the identified dispersion trend where the energy accumulation shows a high peak indicating a high confidence. Then, starting and ending frequencies were assigned to represent the frequency range of dispersion curve to be extracted. A frequency interval of 1 Hz was assigned for the extraction. Dispersion curve extracted by the program usually followed the identified trend. However, it sometimes contained some erroneous portions caused by either broken coherency or adjacent higher mode trends (Park et al., 1999b) or both. In this case, those portions were manually edited by replacing them with those subjectively determined (Figure 5). This manual editing often involved extension of analyzed frequency range by adding more

points (subjectively determined) outside the low and high ends of the original frequency range specified for the automatic picking process by program. Those shot gathers (for example, record 2001) whose overtone images showed no discernible trend of the fundamental-mode Rayleigh waves were discarded from the analysis.

Two passes of dispersion-curve extraction were made. One (to be called "Subjective" analysis) involved the extraction with as much subjective judgment as possible (Figure 6a). This aimed at the maximization in the total number of curves extracted and in the frequency range of each extracted curve. This type of extraction involved examination of an overtone image several times with different parameters of processing and display to gain a subjective idea of how the signal curve might look. Another pass of extraction (to be called "Objective" analysis) involved only those shot gathers whose overtone images show the trend that could be clearly and obviously identified as the fundamental-mode curve (for example, record 2133) (Figure 6b). Dispersion curves extracted from each pass of analysis are displayed in Figure 7.

## Post-Compaction Analysis

Overtone images of all shot gathers collected are displayed in Appendix IV. Overall procedure of the curve extraction was the same as in the pre-compaction case previously outlined. Two passes of Subjective and Objective analyses were made (Figure 8).

## DATA PROCESSING — INVERSION FOR Vs PROFILES

Each dispersion curve was inverted by using an iterative inversion algorithm (incorporated in SurfSeis) by Xia et al. (1999) to produce a one-dimensional (1-D) Vs profile in which vertical variation of Vs at a certain location in the survey line is represented by a layer model (Figure 9). The surface location of a 1-D Vs profile is determined as the middle point of receiver spread used during the dispersion-curve extraction. Each extracted and saved curve contains this information. A 10-layer model with a varying thickness (increasing thickness with depth) was used. This layer model was determined by the program (SurfSeis) based on the relationship between phase velocities and wavelengths calculated from corresponding dispersion curve. Iterative inversion process stopped when one of the three criteria was met whichever came first: 1) when overall root-mean-square error (RMS-E) dropped below 10., or 2) when total iteration reached thirty times, or 3) when change of RMS-E remained less than five percent for successive five iterations (SurfSeis Users' Manual, 2003).

## Pre-Compaction 2-D Vs Map

Two 2-D Vs maps were constructed: one (Subjective Vs map) (Figure 10a) by using the 1-D Vs profiles obtained from all the Subjective dispersion curves and another (Objective Vs map) (Figure 11a) by using 1-D Vs profiles obtained from all the Objective curves. Location of each 1-D Vs profile used for the construction of the map is indicated by a triangular mark at the bottom of map. Corresponding RMS-E maps of Figures 10b

and 11b, respectively, indicate relative confidence level (the smaller RMS-E, the higher confidence) of the corresponding portion in the 2-D Vs maps. Since this confidence was calculated purely from the numerical perspectives, they should be used with a care.

**Post-Compaction 2-D Vs Map**

Same procedure was taken as in the pre-compaction case to produce the 2-D Vs maps: Subjective (Figure 12a) and Objective (Figure 13a) maps. Corresponding RMS-E maps are also displayed in Figures 12b and 13b, respectively.

## DISCUSSIONS

General Vs trends observed in both pre- and post-compaction 2-D Vs maps indicate that there is a significant horizontal change in elastic property of soil at locations around 2130 (in pre-compaction map) and 4090 (in post-compaction map). While there is a distinctive interface at depth of about 10 ft with a zone of lower Vs overlying another zone of higher Vs for the zone preceding these two stations, the interface disappears quite abruptly afterward. Therefore, it would be reasonable to compare Vs results by correlating these two locations as a common reference point and discuss the Vs changes in these two zones: one before (Zone 1) and another (Zone 2) after this reference point (Figures 10-13).

Comparing Vs maps from Subjective and Objective analyses, the Objective Vs maps are seen as slightly smoothed versions of the Subjective ones. This is because of the lesser number of data points used during the inversion process. Therefore, it can be said that the Objective maps have a lesser degree of resolution in both horizontal and vertical directions. For example, the abrupt and unrealistic horizontal step-like change observed at the boundary between Zone 1 and Zone 2 in the pre-compaction Objective Vs map (Figure 11a) is due to the lack of dispersion curves used. However, since those lesser number of data points were picked from the most objective standards, it can also be said that the general trend of Vs variation in the Objective maps may have a higher confidence than in the Subjective maps. This is indicated by RMS error maps showing that overall error values were reduced in the case of the Objective analysis. Therefore, comparison of both types of maps should be accompanied with a discreet account of these aforementioned aspects.

Comparing Vs maps from pre- and post-compaction data, no discernible change is observed for Zone 1. Zone 2, however, indicates that there is a significant reduction in Vs for most of depth range (0-25 ft). Soils (Part A) with S-velocity (Vs) lower than 200 ft/sec observed only at depths shallower than 5 ft in the pre-compaction maps (white-colored area in Figures 10a and 11a) are now observed to have extended down to about 10 ft depth in the post-compaction maps of Figures 12a and 13a, respectively. In addition, those portions of soil (Part B) with Vs of about 500 ft/sec are observed to have extended down to the maximum depth (25 ft) investigated.

Reduction of Vs observed in some parts of the soil is believed due to the loss of cohesive bonding between soil particles that was established throughout a prolonged time period (Whitlow, 1995).

## CONCLUSIONS

It is concluded that shear-velocity (Vs) for certain parts of the soil became reduced after the Deep Dynamic Compaction (DDC) operations had been applied. The reduction occurred in depth ranges of 5-10 ft and 15-25 ft in the surveyed area.

## REFERENCES CITED


Bullen, K.E., 1963, An introduction to the theory of seismology, 3rd Ed.; Cambridge University Press, London, 381 pp.

Dobrin, M.B., and Savit, C.H., 1988, Introduction to geophysical prospecting, 4th ed.: McGraw-Hill, Inc., New York, 867 pp.

Lunne, T., 1997, Cone penetration testing in geotechnical practice; Blackie Academic & Professional, London, 312 pp.

Miller, R.D., Xia, J., Park, C.B., and Ivanov, J., 1999, "Multichannel analysis of surface waves to map bedrock," *The Leading Edge*, 18(12), 1392-1396.

Park, C.B., Miller, R.D., and Miura, H., 2002, Optimum field parameters of an MASW survey [Exp. Abs.]: SEG-J, Tokyo, May 22-23, 2002.

Park, C.B., Miller, R.D., and Xia, J., 2001, Offset and resolution of dispersion curve in multichannel analysis of surface waves (MSW): Proceedings of the SAGEEP 2001, Denver, Colorado, SSM-4.

Park, C.B., Miller, R.D., and Xia, J., 1999a, "Multi-channel analysis of surface waves," *Geophysics*, 64(3), 800-808.

Park, C.B., Miller, R.D., Xia, J., Hunter, J.A., and Harris, J.B., 1999b, Higher mode observation by the MASW method [Exp. Abs.]: Soc. Explor. Geophys., p. 524-527.

Park, C. B., Xia, J., and Miller, R. D., 1998, Imaging dispersion curves of surface waves on multi-channel record: 68th Ann. Internat. Mtg., Soc. Expl. Geophys., Expanded Abstracts, 1377–1380.

Richart, F. E., Hall, J. R., and Woods, R. D., 1970, Vibrations of soils and foundations: Prentice-Hall, Inc., 414 pp.

Sheriff, R.E., and Geldart, L.P., 1982, Exploration seismology, volume 1: Cambridge University Press, 253 pp.

Stokoe II, K. H., Wright, S.G., Bay, J.A., and Roesset, J.M., 1994, Characterization of geotechnical sites by SASW method, in Geophysical characterization of sites, ISSMFE Technical Committee #10, edited by R. D. Woods, Oxford Publishers, New Delhi.

SurfSeis v. 1.5, 2003, Users' Manual; Kansas Geological Survey, Lawrence, Kansas.

Telford, W.M., Geldart, L.P., Sheriff, R.E., and Keys, D.A., 1976, Applied Geophysics, Cambridge University Press, Cambridge, 860 pp.

Xia, J., Miller, R.D., and Park, C.B., 1999, "Estimation of near-surface shear-wave velocity by inversion of Rayleigh wave," *Geophysics*, 64(3), 691-700.

Whitlow, R., 1995, Basic soil mechanics (3rd Ed.); Longman Scientific & Technical, Essex, England, 559 pp.

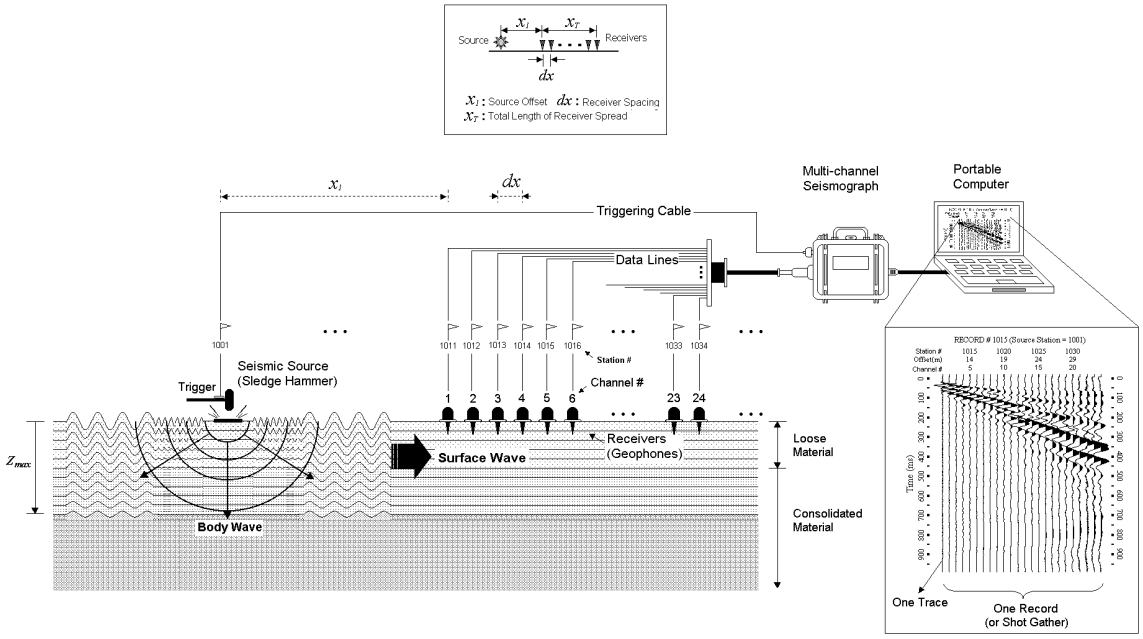


Figure 1. A schematic illustrating a typical field configuration with a MASW survey.

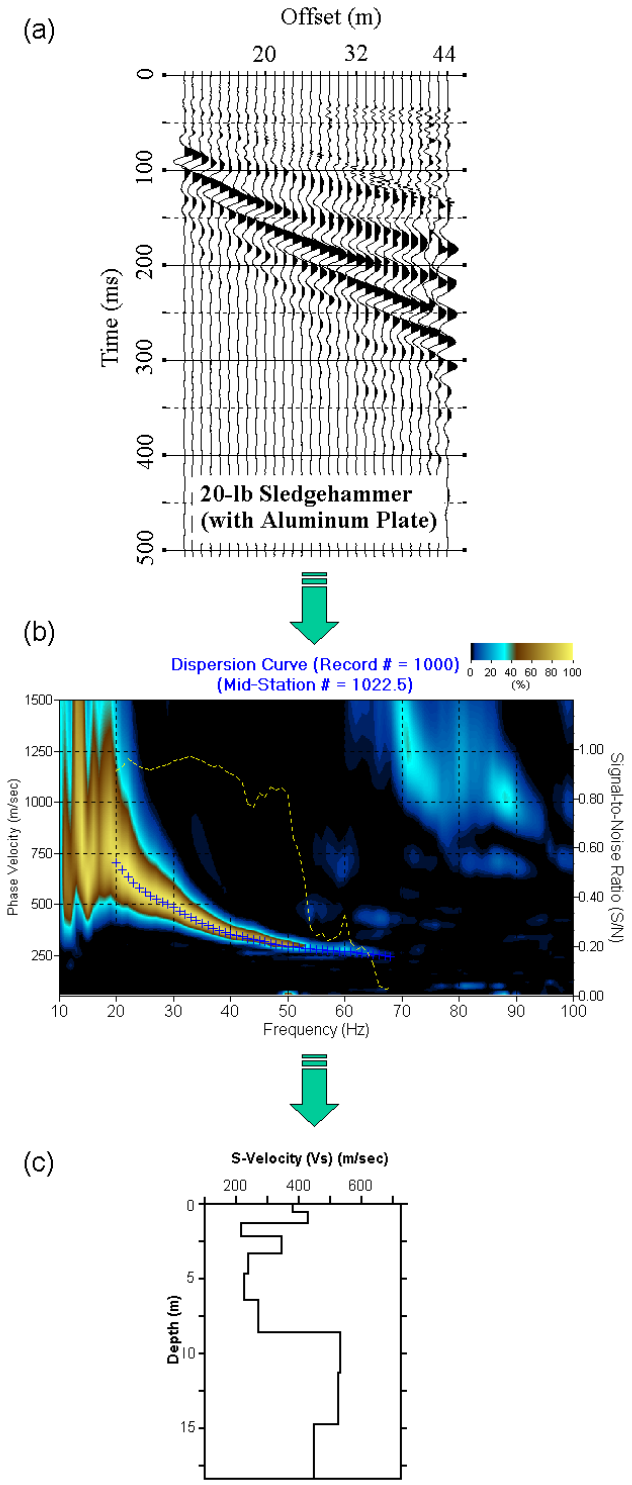


Figure 2. General procedure of a MASW processing; a multichannel record (shot gather) in (a) is transformed into (b) an overtone image in which the fundamental-mode dispersion is identified and corresponding signal curve is extracted, and then (c) the curve is inverted into a 1-D Vs profile.

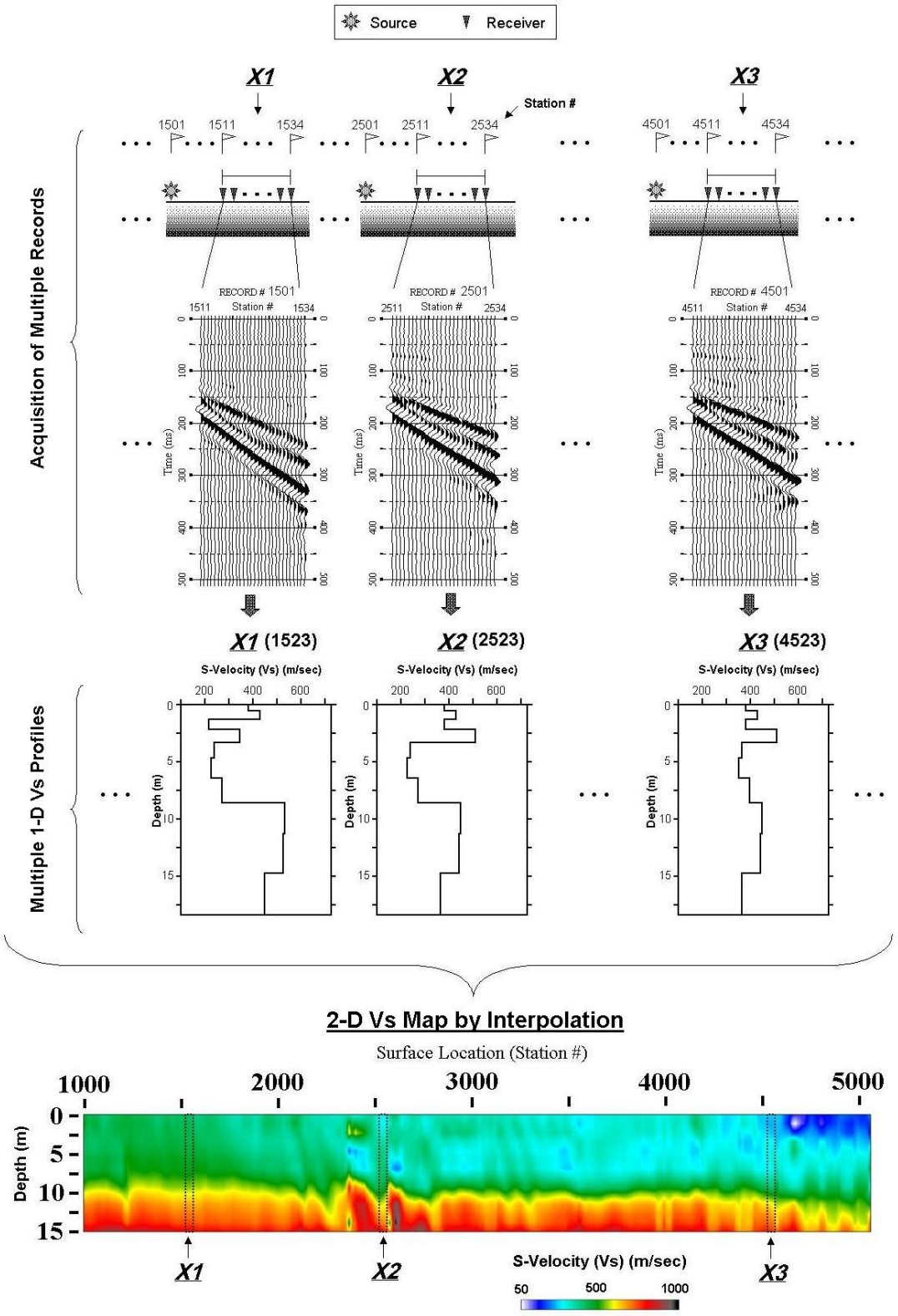


Figure 3. Illustration of the procedure to generate a 2-D Vs map from a roll-along mode MASW survey.

(a)

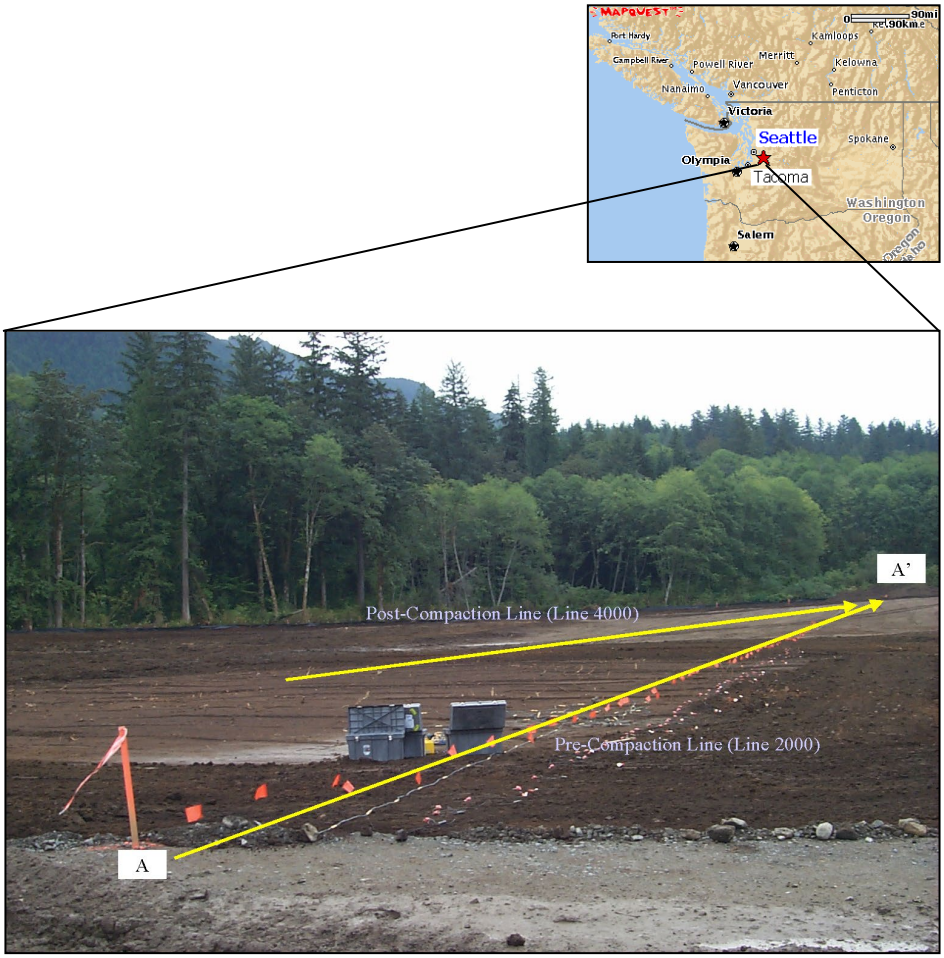


(b)

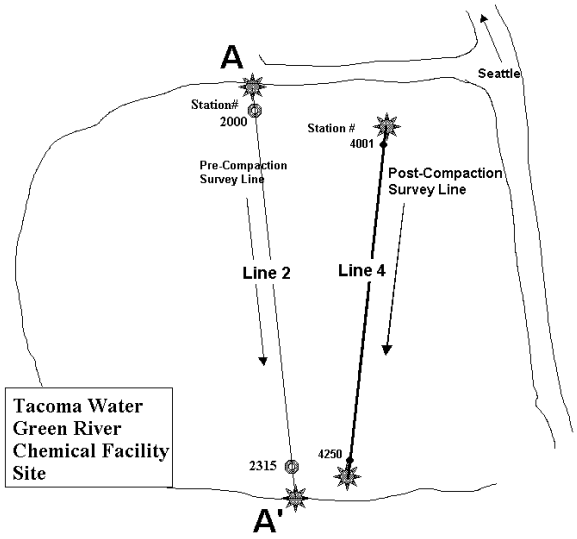


Figure 4. (a) Location map of the site and (b) schematic of the two survey lines.

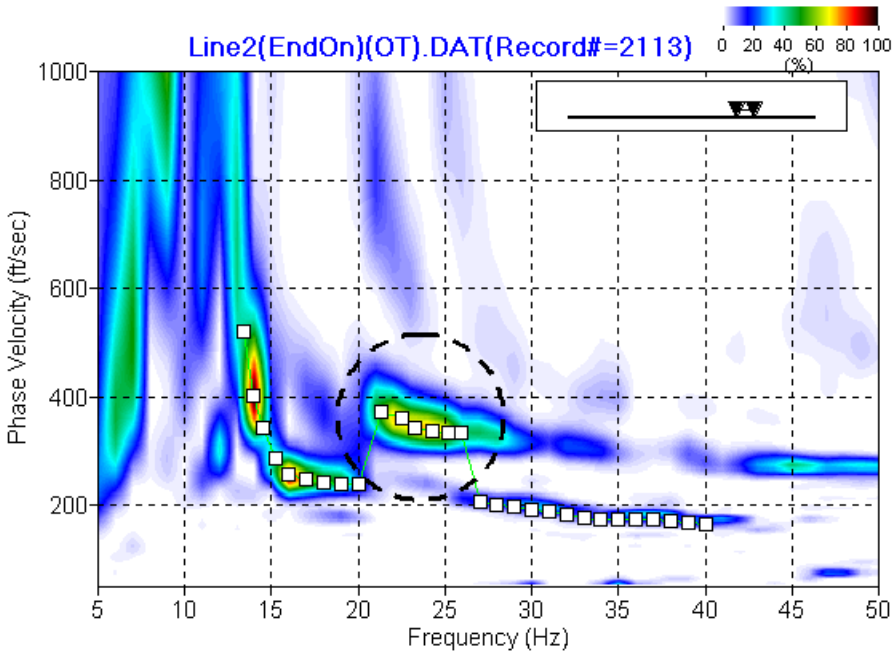


Figure 5. An example of dispersion curve extraction by using SurfSeis that shows a higher mode adjacent to the fundamental mode causes some erroneous picking of phase velocities. The pickings are then manually edited.

(a)

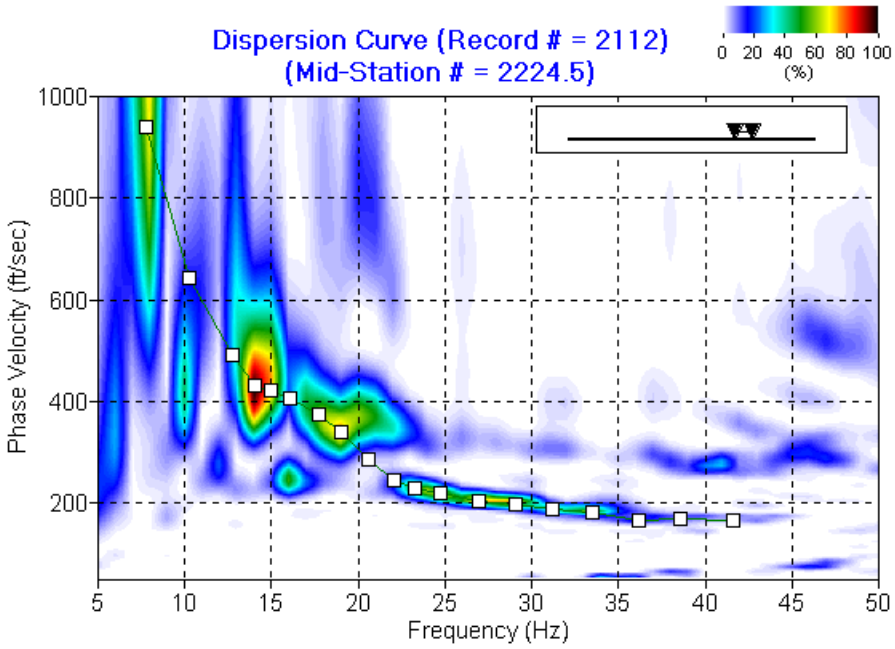


(b)

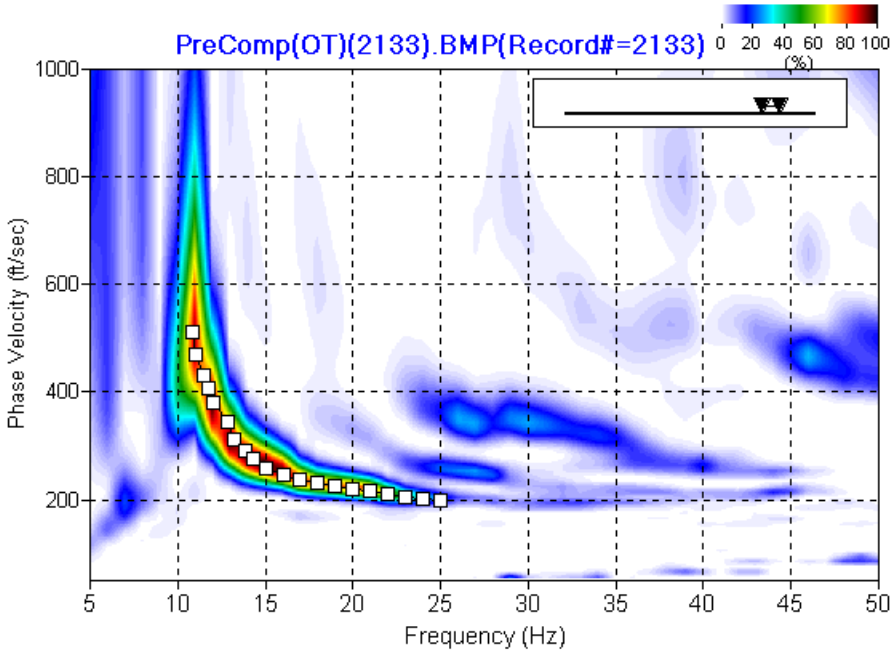


Figure 6. Examples of dispersion curve extraction based on the overtone image; (a) a curve is extracted with as much subjective judgement involved as possible (Subjective analysis) and (b) only by the objective trend of dispersion (Objective analysis).

(a)

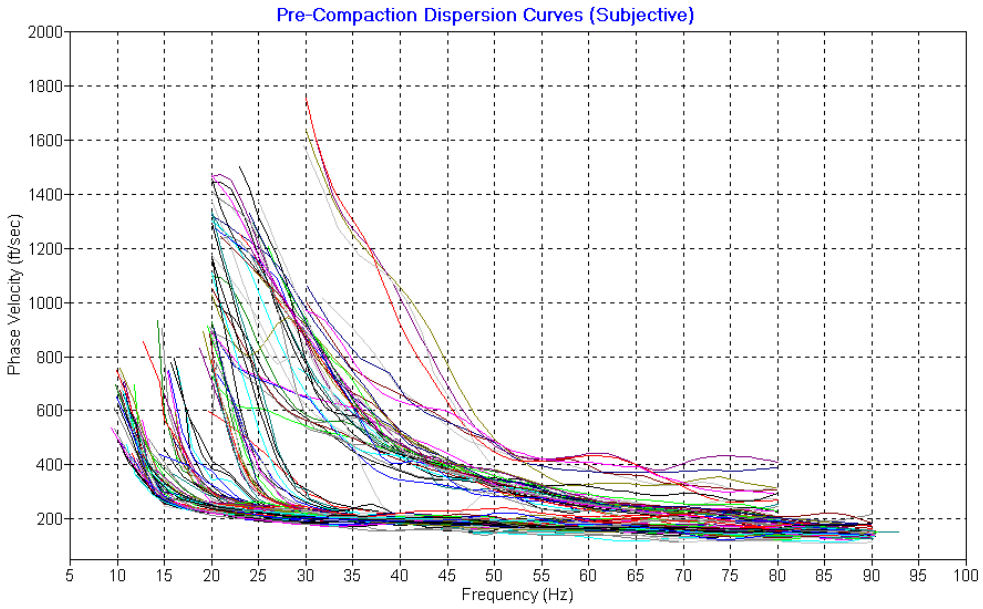


(b)

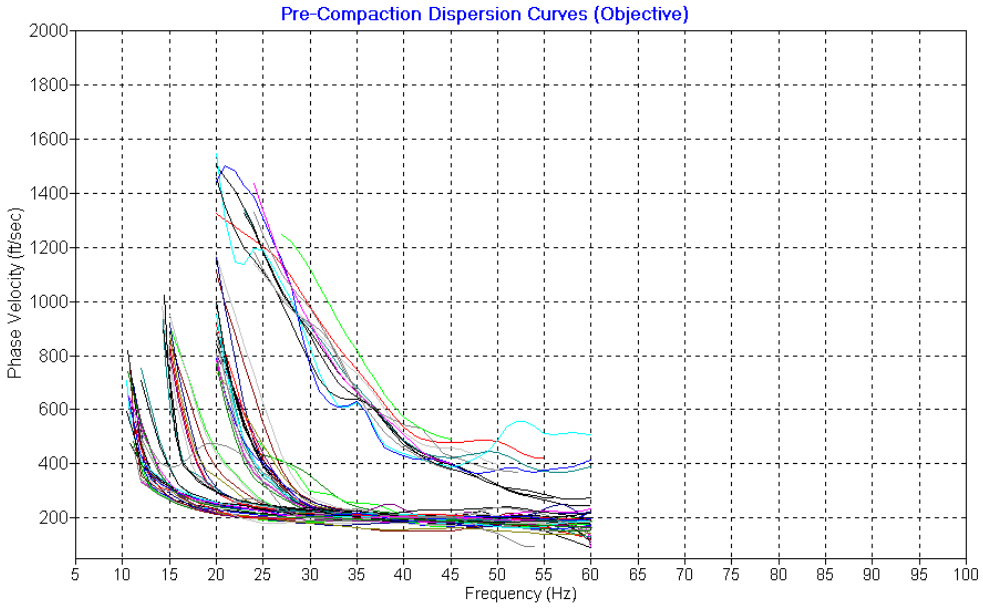


Figure 7. Display of dispersion curves extracted from (a) the Subjective and (b) the Objective analyses of the pre-compaction (line 2000) data.

(a)

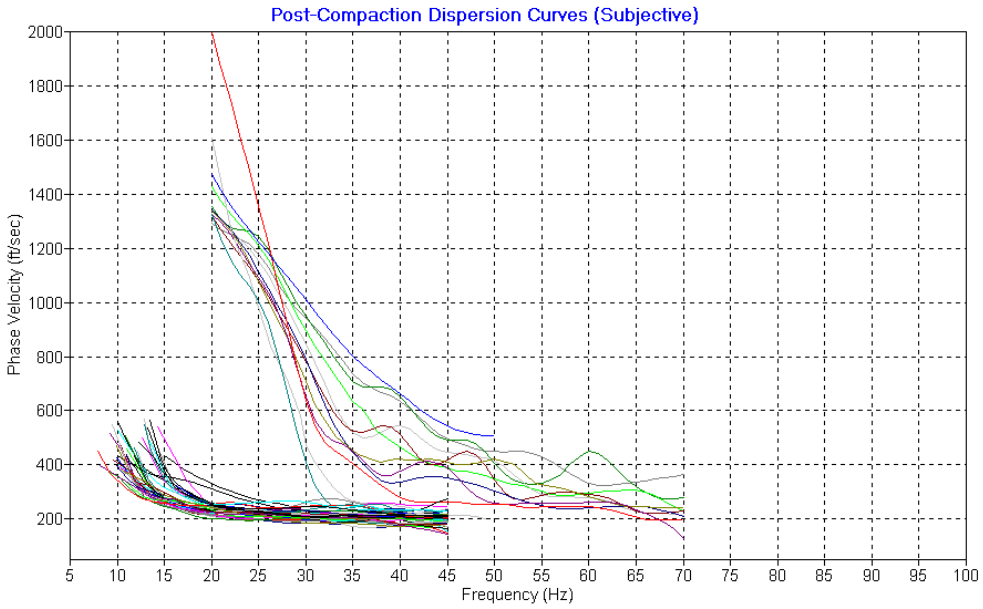


(b)

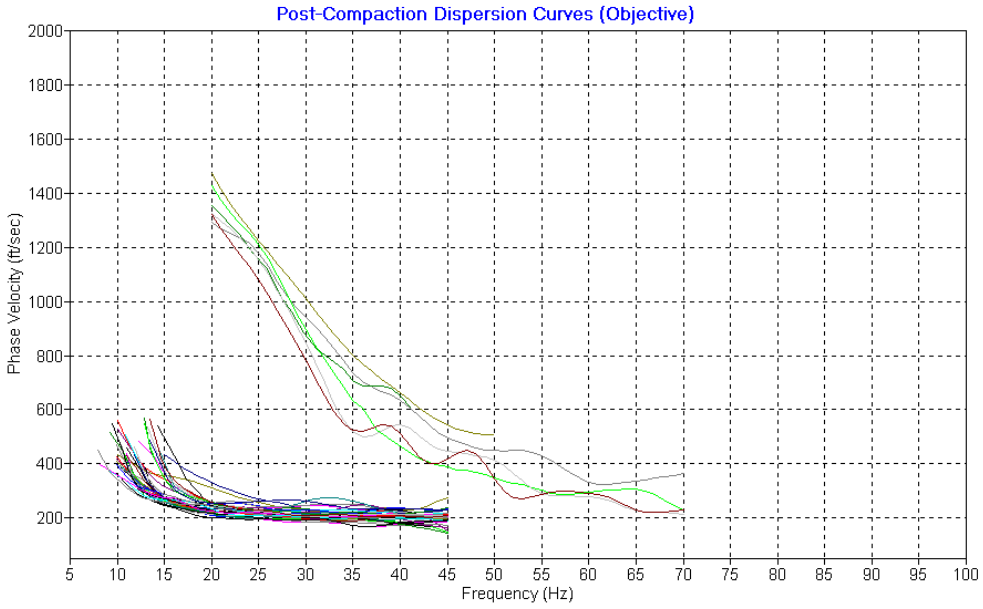


Figure 8. Display of dispersion curves extracted from (a) the Subjective and (b) the Objective analyses of the post-compaction (line 4000) data.

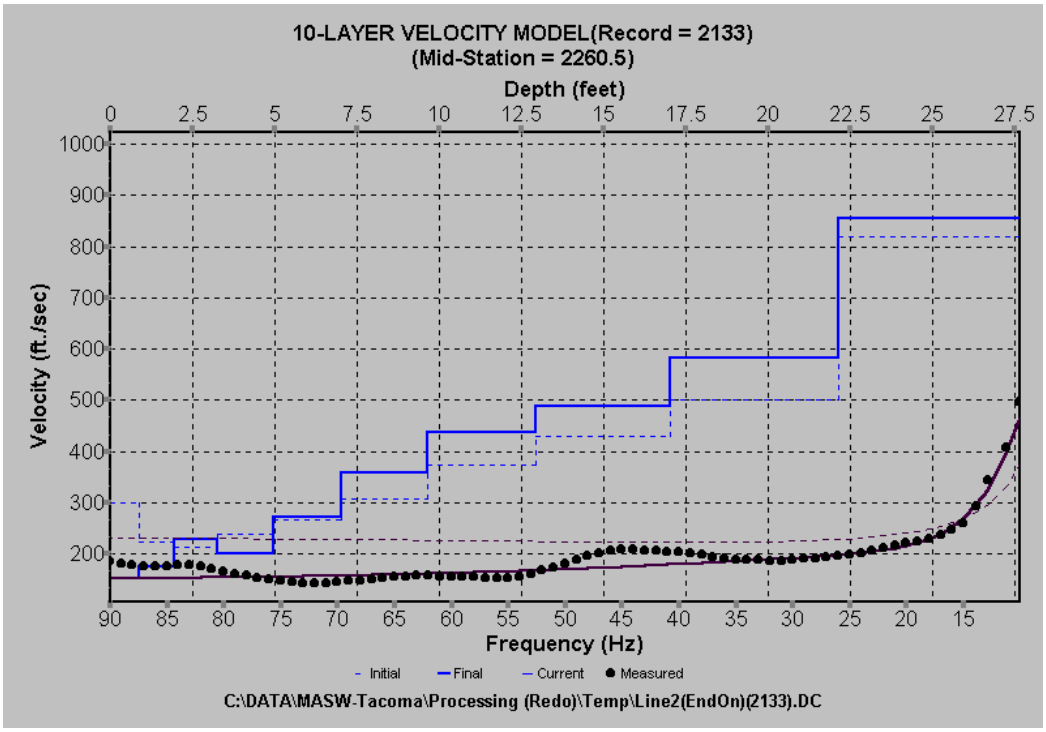


Figure 9. An example of inversion for a 1-D Vs profile in which a 10-layer depth model is created with varying thickness (increasing with depth) determined from the input dispersion curve (represented by dots).

(a)

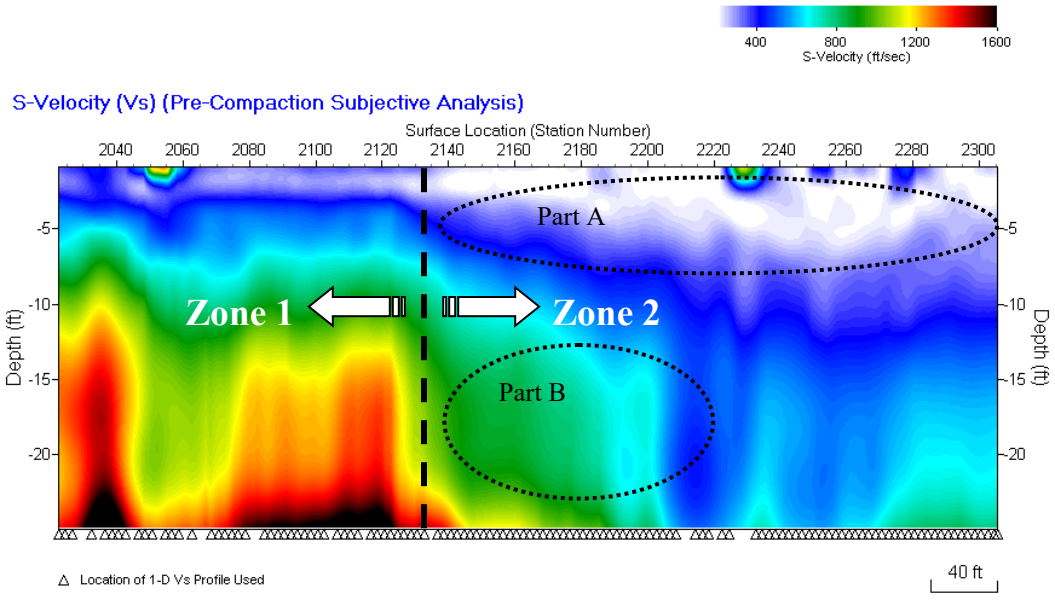


(b)

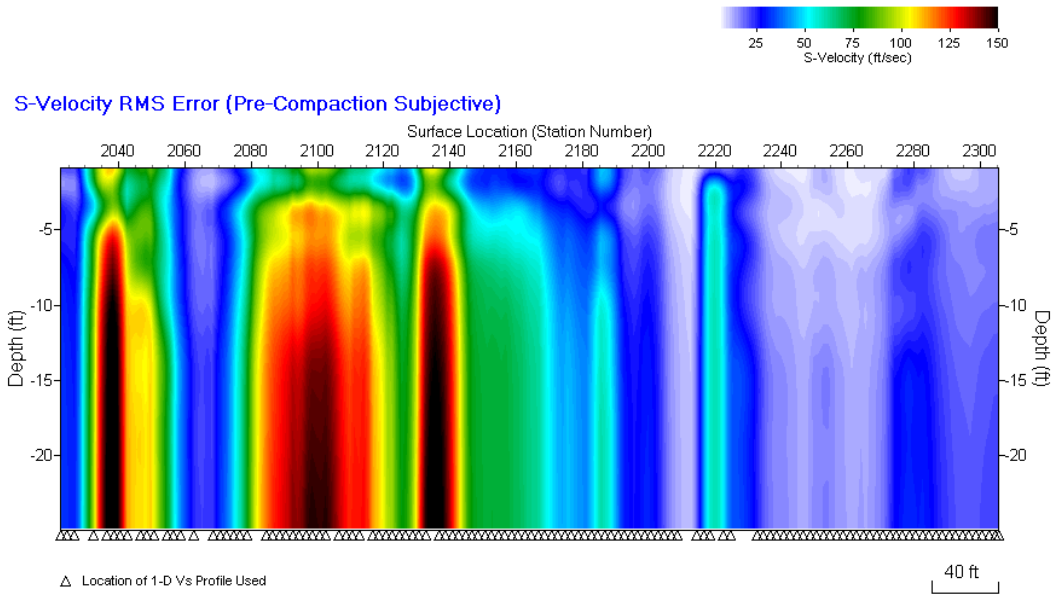


Figure 10. (a) Pre-compaction Vs map constructed from the inversion of all Subjective dispersion curves and (b) corresponding RMS-Error map.

(a)

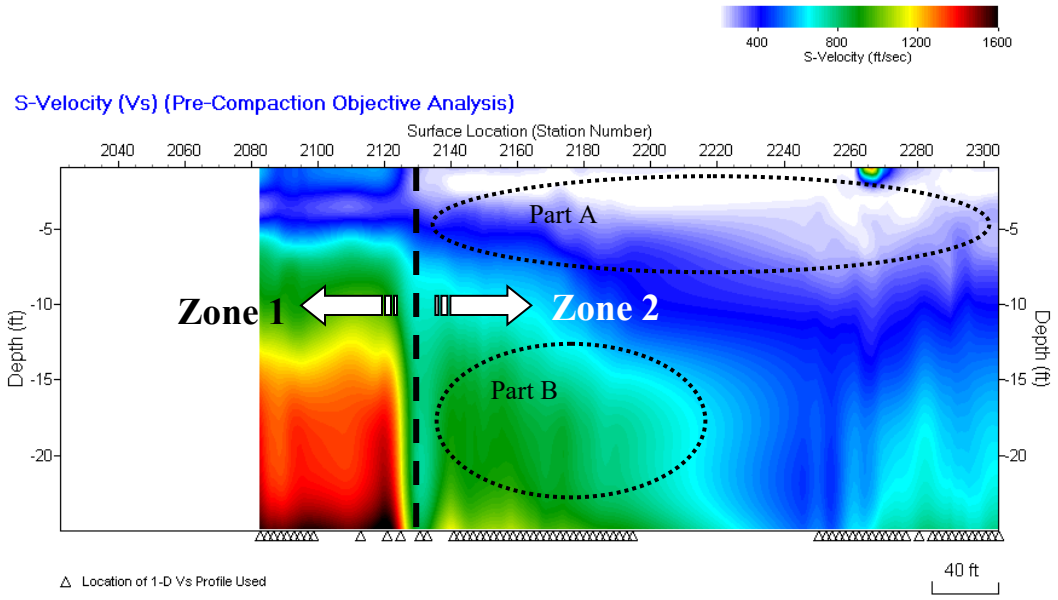


(b)

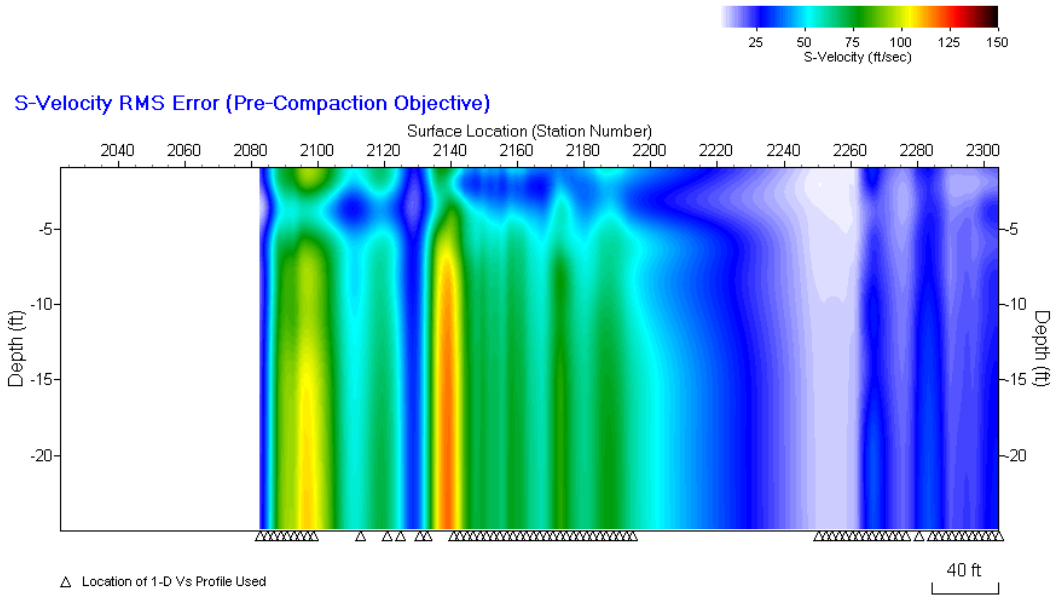


Figure 11. (a) Pre-compaction Vs map constructed from the inversion of all Objective dispersion curves and (b) corresponding RMS-Error map.

(a)

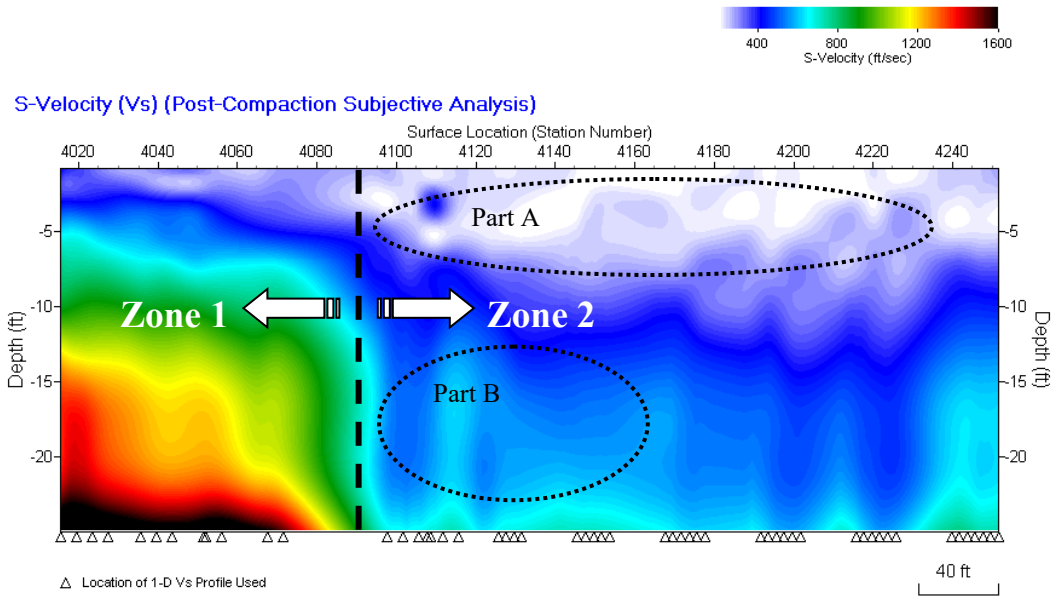


(b)

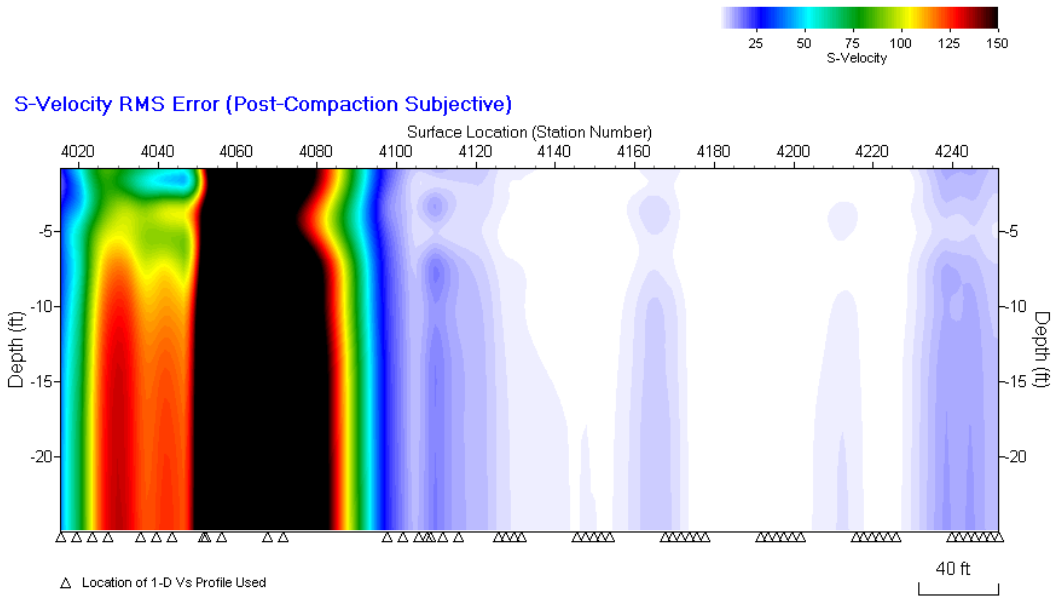


Figure 12. (a) Post-compaction Vs map constructed from the inversion of all Subjective dispersion curves and (b) corresponding RMS-Error map.

(a)

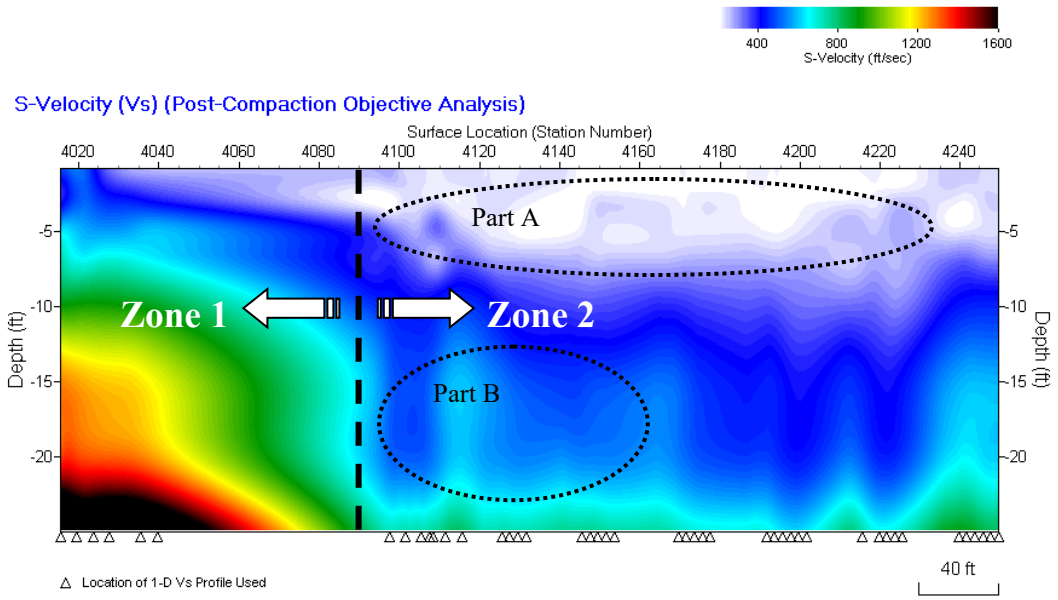


(b)

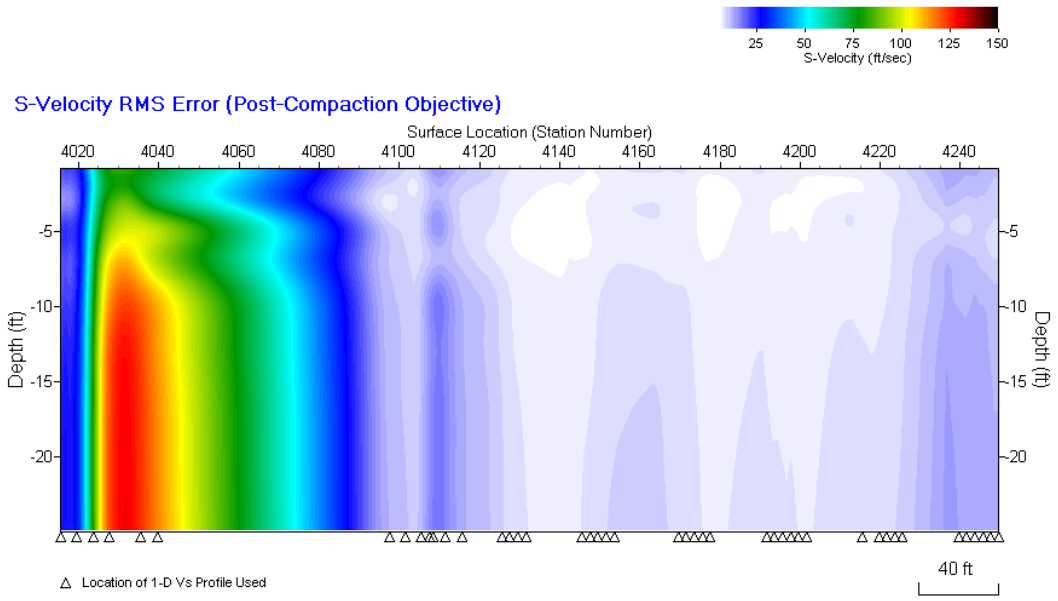


Figure 13. (a) Pre-compaction Vs map constructed from the inversion of all Objective dispersion curves and (b) corresponding RMS-Error map.

# APPENDICES

# to

# KGS Open-File Report (2003-64)

# " MASW for Shear Wave Velocity Evaluation of Soil Before and After Deep Dynamic Compaction Operations"

by

Choon B. Park and Richard D. Miller

Kansas Geological Survey
University of Kansas
1930 Constant Avenue, Campus West
Lawrence, Kansas 66047-3726
Tel: 785-864-2162  Fax: 785-864-5317
Emails: park@kgs.ku.edu, rmiller@kgs.ku.edu

## APPENDIX I

Display of seismic shot gathers from pre-compaction survey

## APPENDIX II

Display of seismic shot gathers from post-compaction survey

## APPENDIX III

Display of overtone images from pre-compaction seismic shot gathers

## APPENDIX IV

Display of overtone images from post-compaction seismic shot gathers

# APPENDIX I

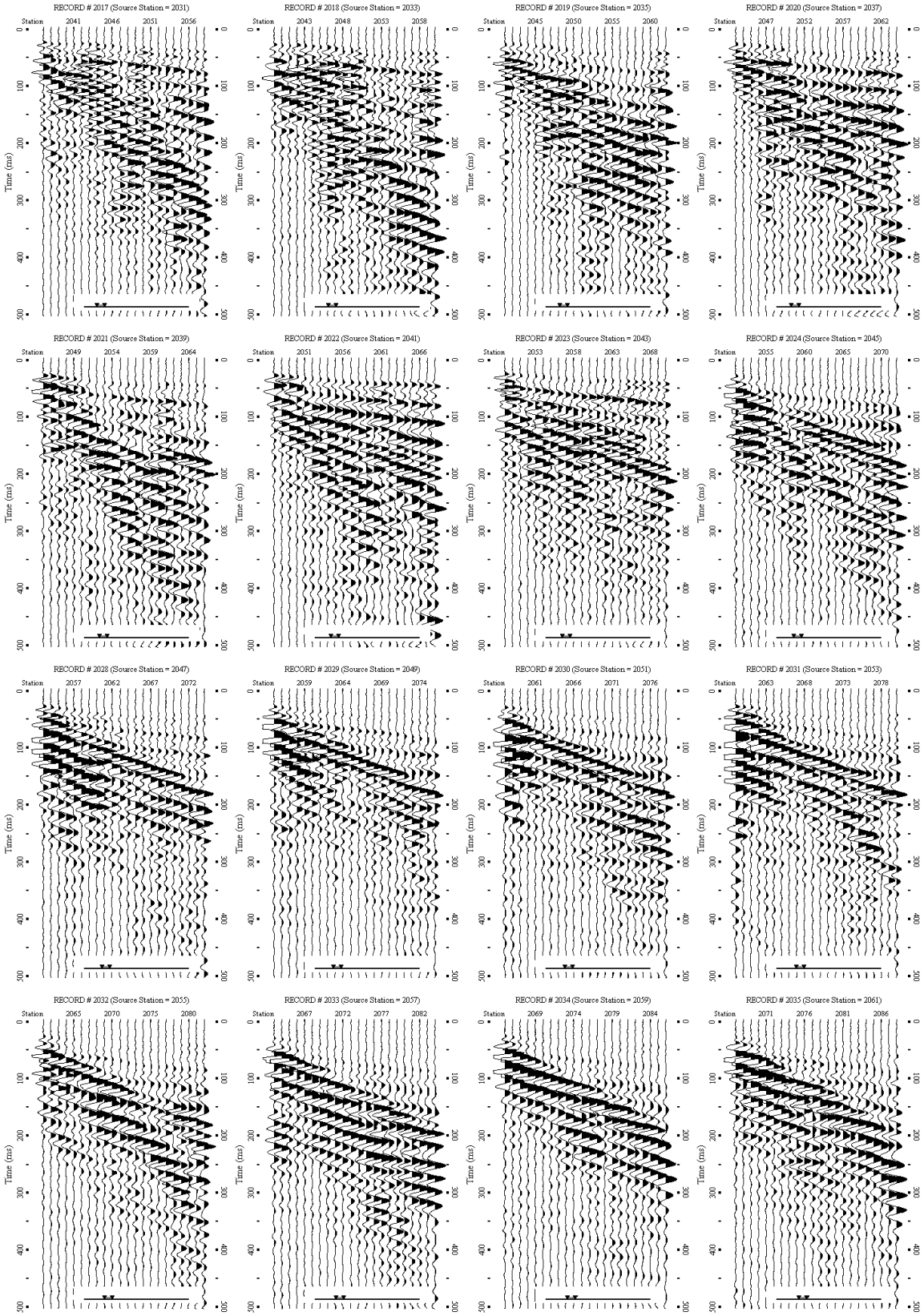
RECORD # 2017 (Source Station = 2031)
RECORD # 2018 (Source Station = 2033)
RECORD # 2019 (Source Station = 2035)
RECORD # 2020 (Source Station = 2037)
RECORD # 2021 (Source Station = 2039)
RECORD # 2022 (Source Station = 2041)
RECORD # 2023 (Source Station = 2043)
RECORD # 2024 (Source Station = 2045)
RECORD # 2028 (Source Station = 2047)
RECORD # 2029 (Source Station = 2049)
RECORD # 2030 (Source Station = 2051)
RECORD # 2031 (Source Station = 2053)
RECORD # 2032 (Source Station = 2055)
RECORD # 2033 (Source Station = 2057)
RECORD # 2034 (Source Station = 2059)
RECORD # 2035 (Source Station = 2061)
Station
Time (ms)

# **APPENDIX I** (continued)

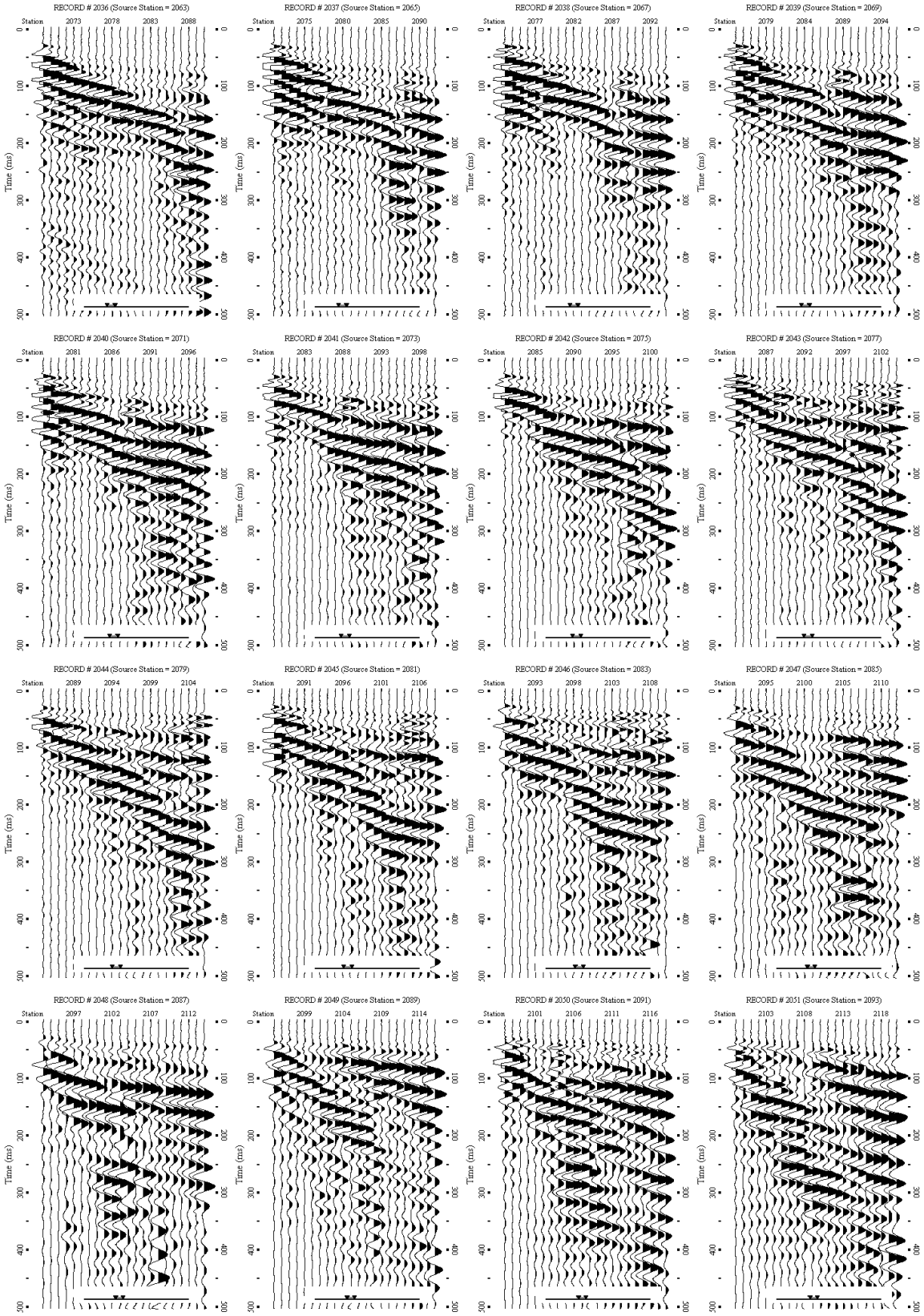

# **APPENDIX I** (continued)

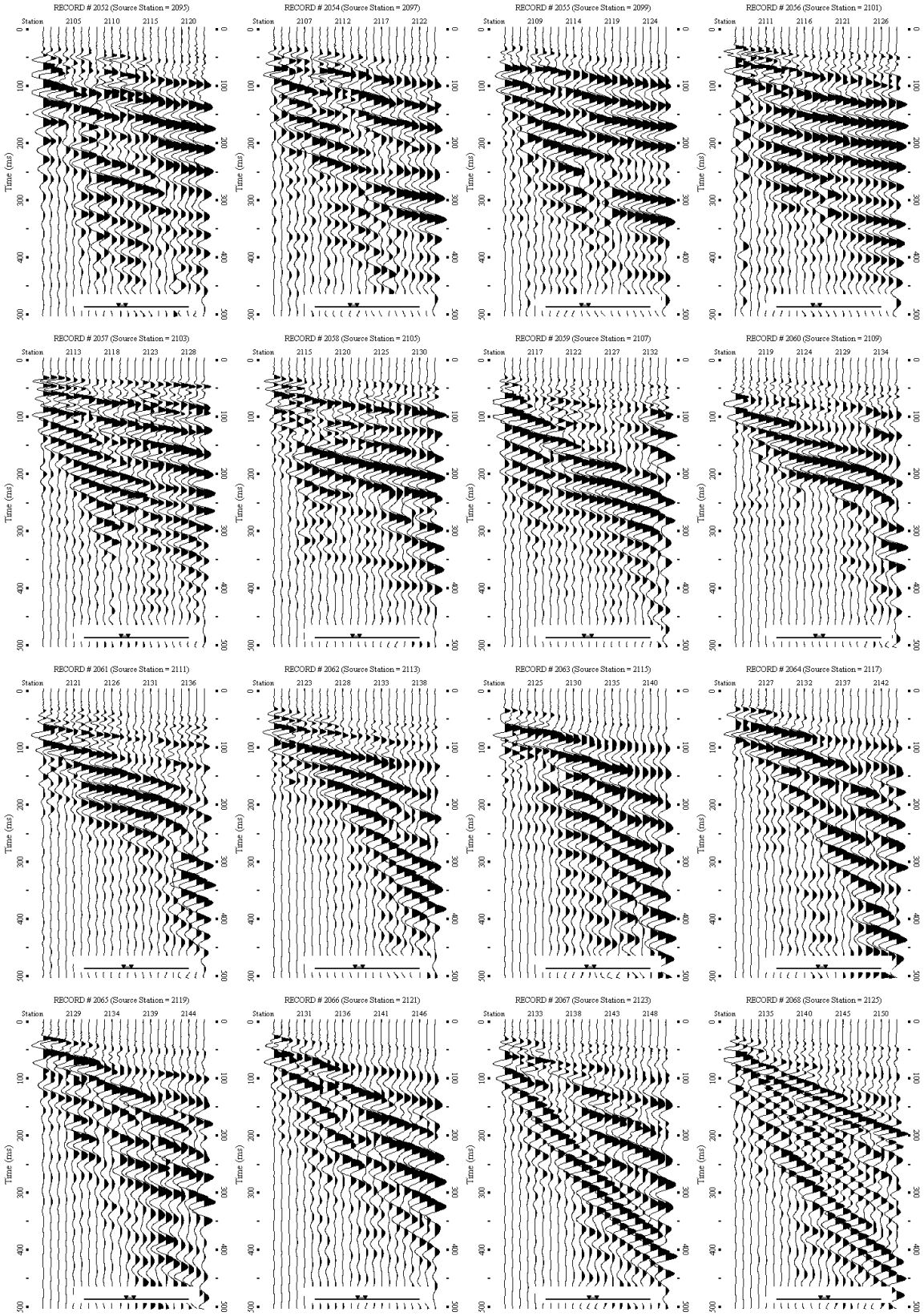

# **APPENDIX I** (continued)

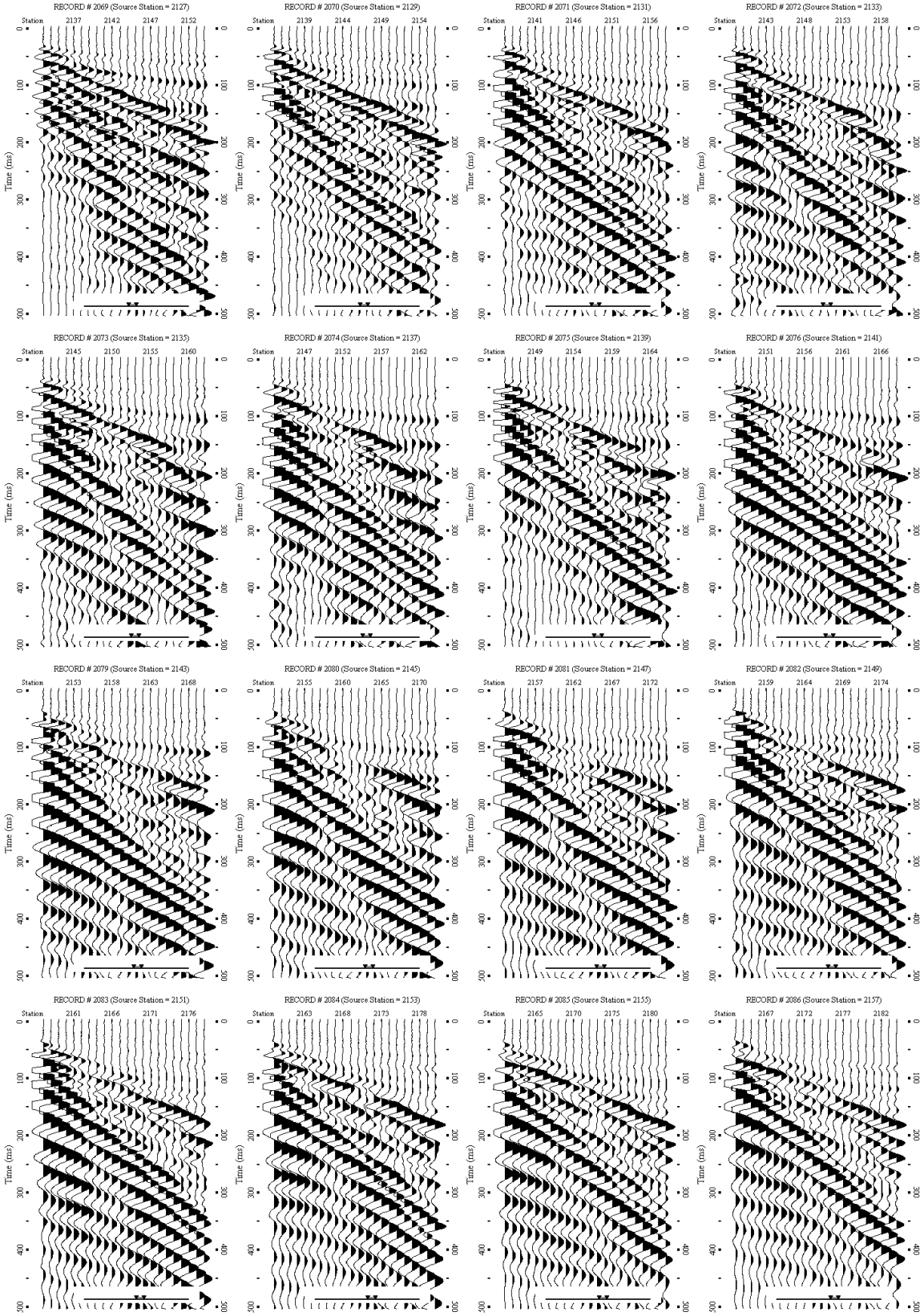

# **APPENDIX I** (continued)

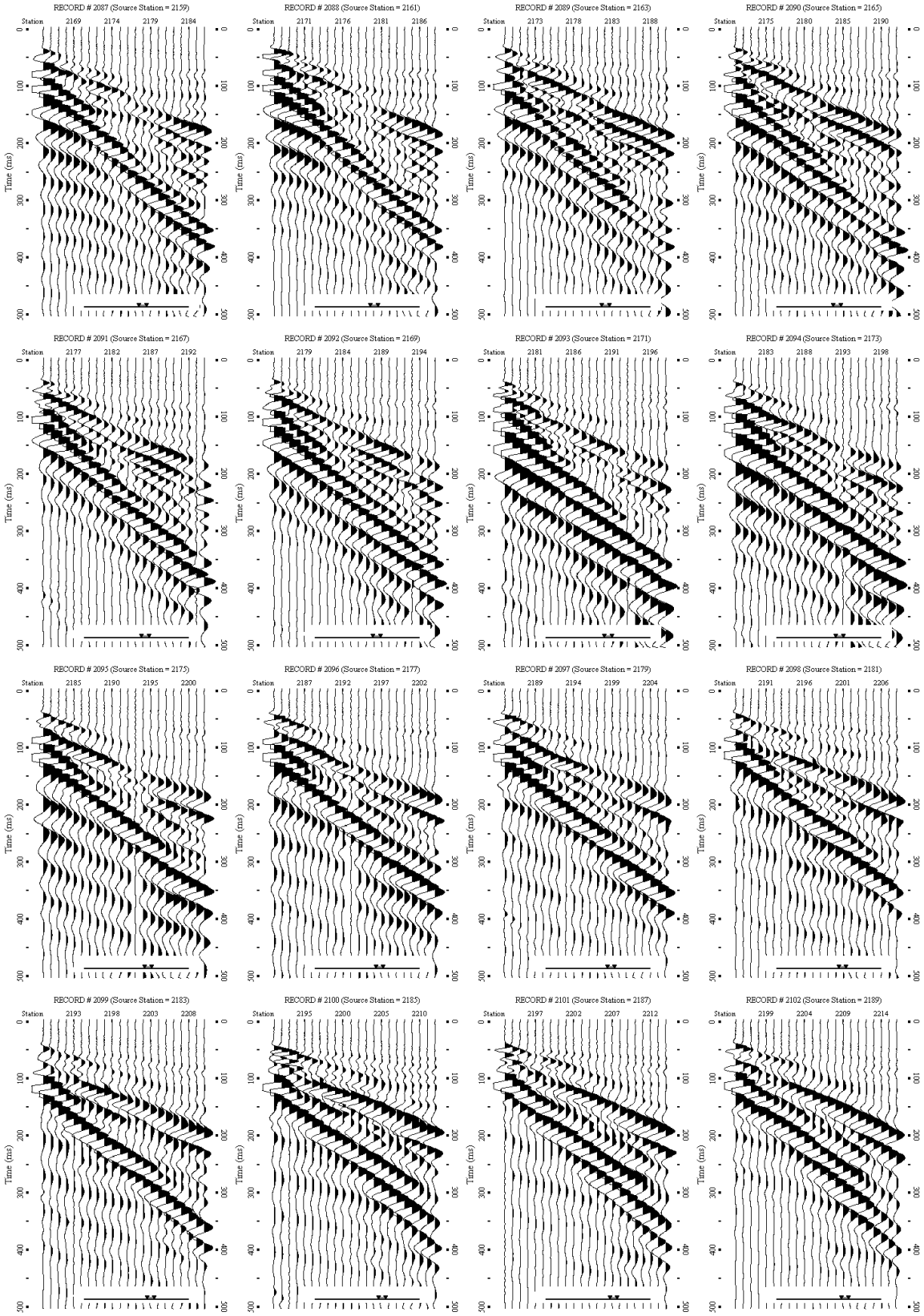

# **APPENDIX I** (continued)

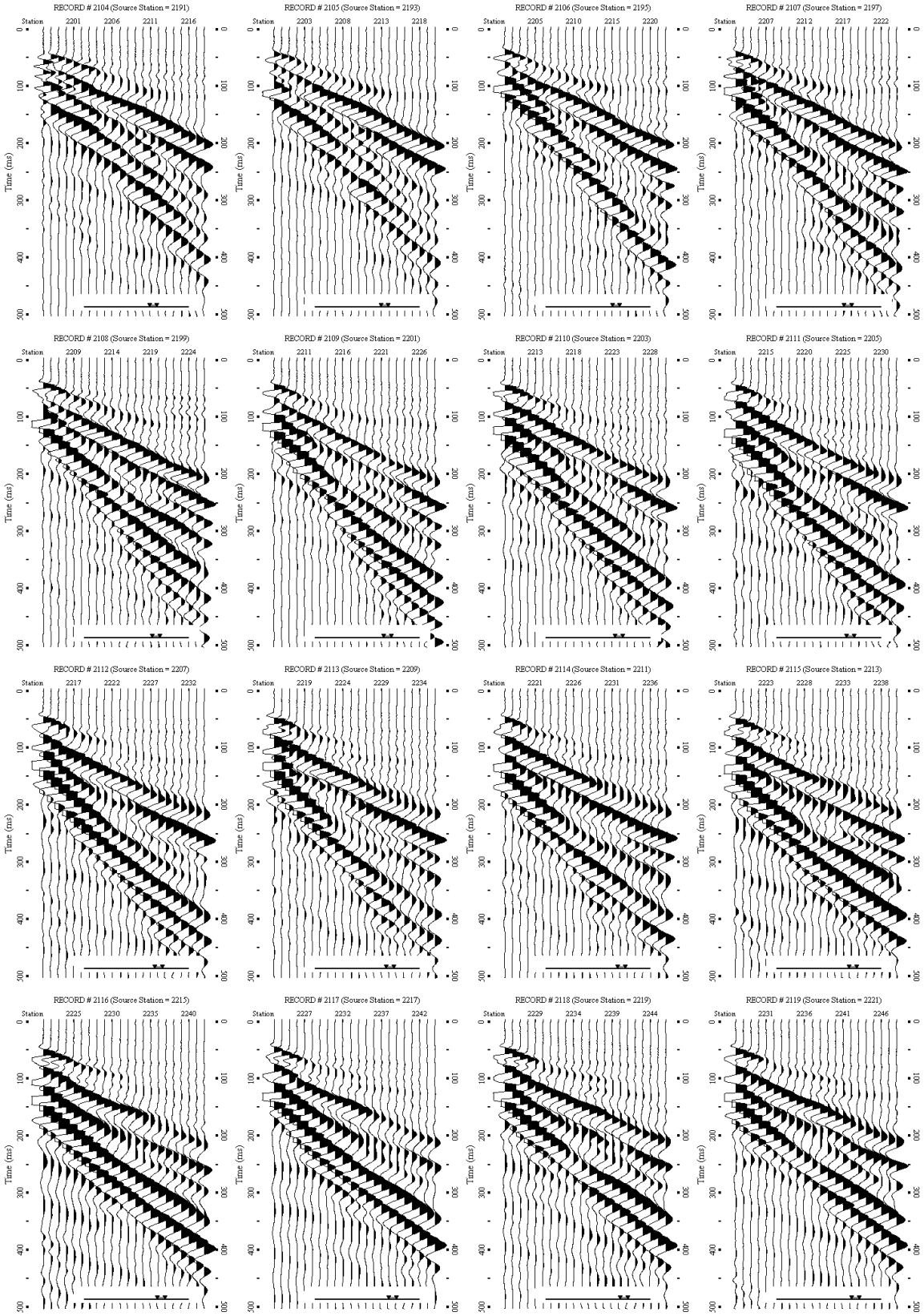

# **APPENDIX I** (continued)

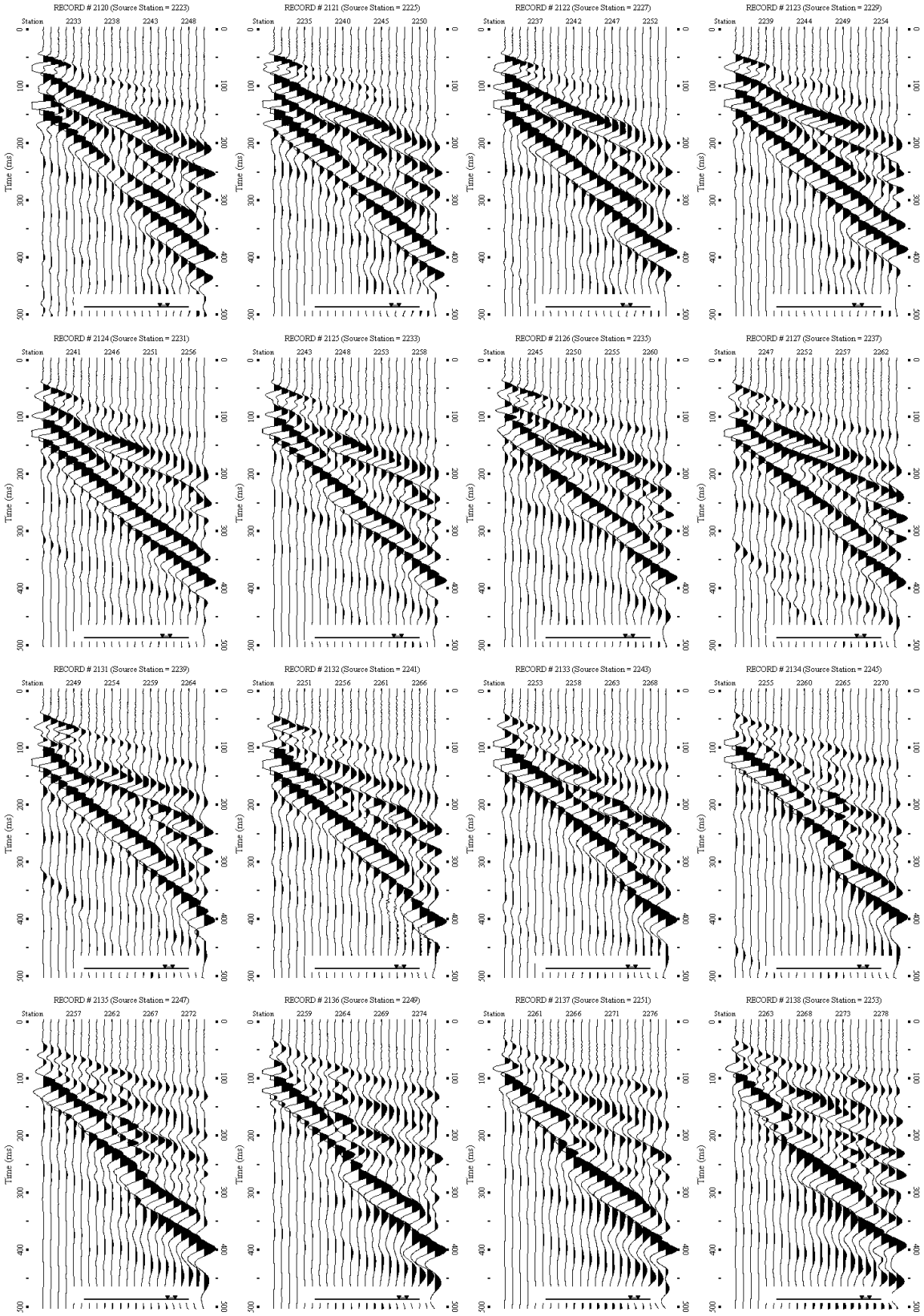

# **APPENDIX I** (continued)

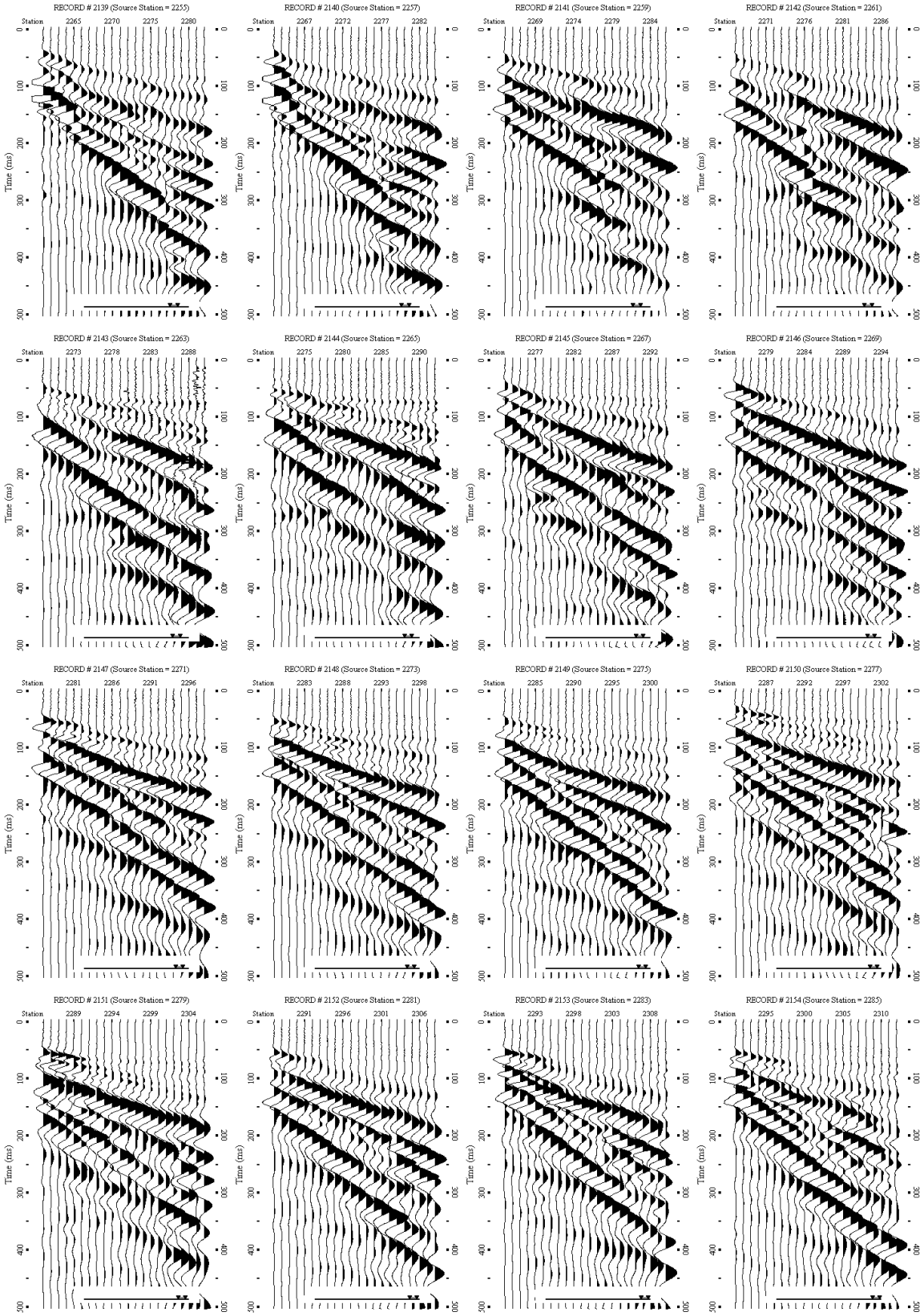

## **APPENDIX I** (continued)

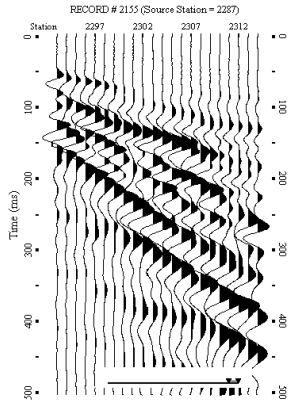

# APPENDIX II

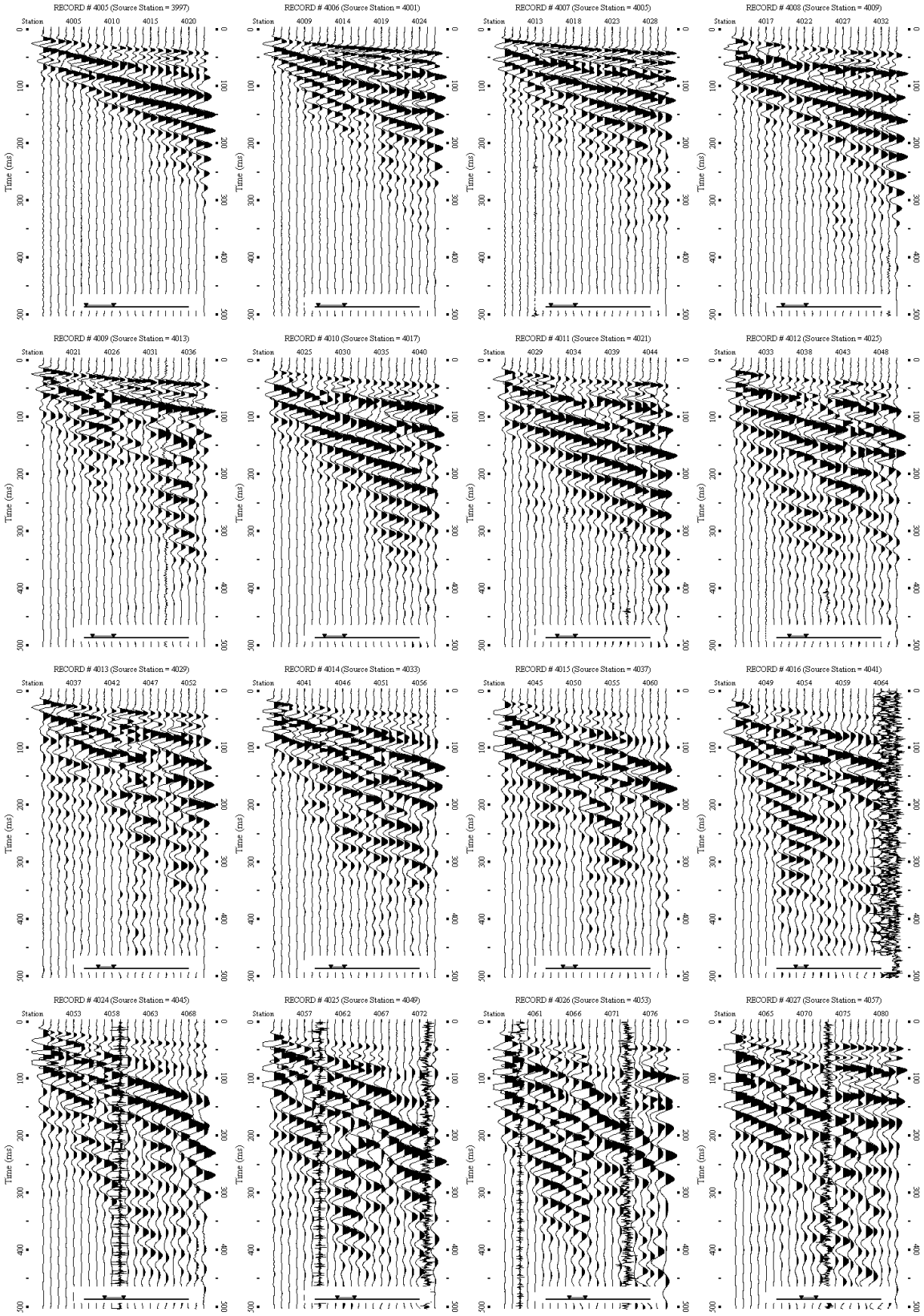
RECORD # 4005 (Source Station = 3997)
RECORD # 4006 (Source Station = 4001)
RECORD # 4007 (Source Station = 4005)
RECORD # 4008 (Source Station = 4009)
RECORD # 4009 (Source Station = 4013)
RECORD # 4010 (Source Station = 4017)
RECORD # 4011 (Source Station = 4021)
RECORD # 4012 (Source Station = 4025)
RECORD # 4013 (Source Station = 4029)
RECORD # 4014 (Source Station = 4033)
RECORD # 4015 (Source Station = 4037)
RECORD # 4016 (Source Station = 4041)
RECORD # 4024 (Source Station = 4045)
RECORD # 4025 (Source Station = 4049)
RECORD # 4026 (Source Station = 4053)
RECORD # 4027 (Source Station = 4057)
Station
Time (ms)

# **APPENDIX II** (continued)

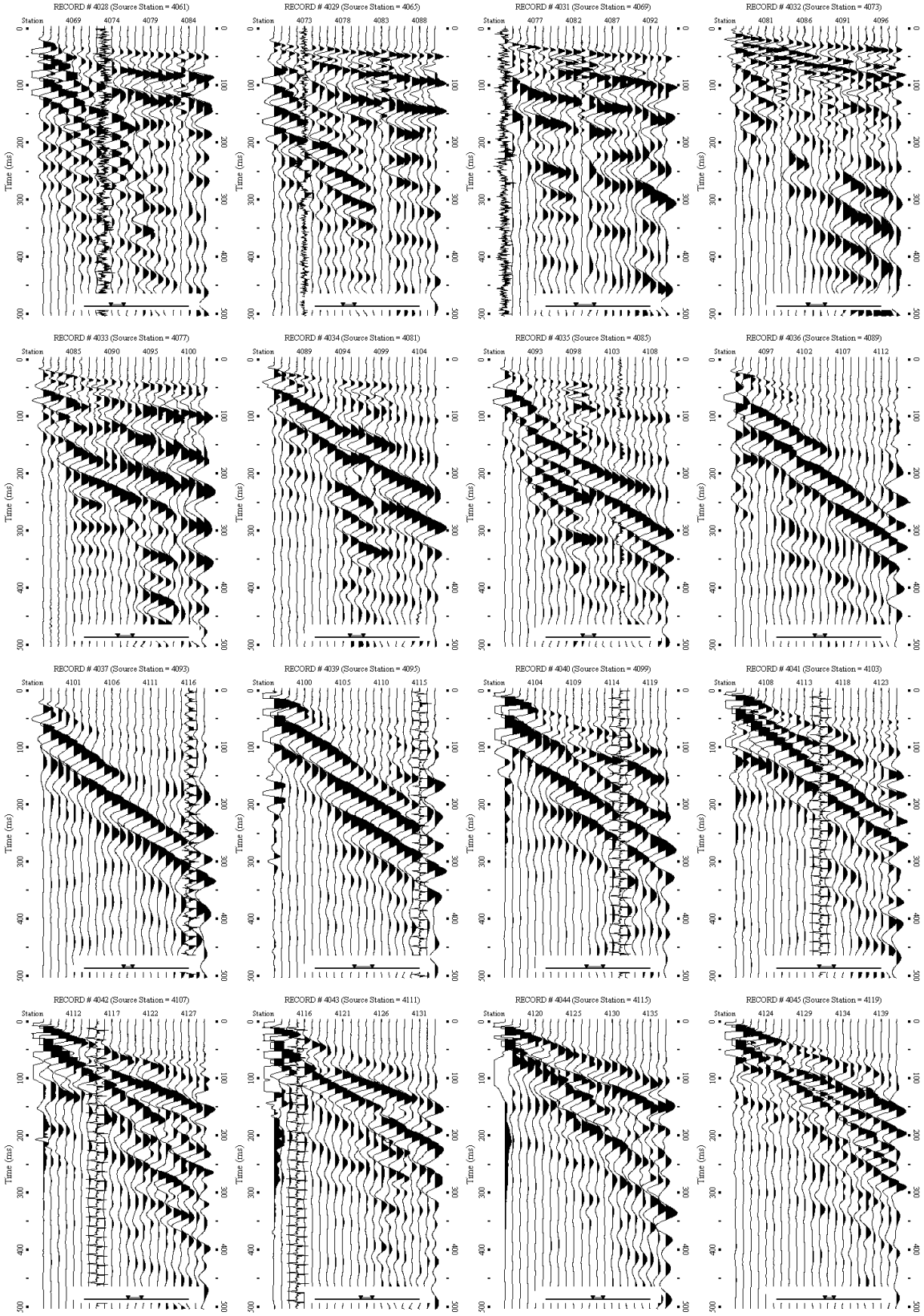

# **APPENDIX II** (continued)

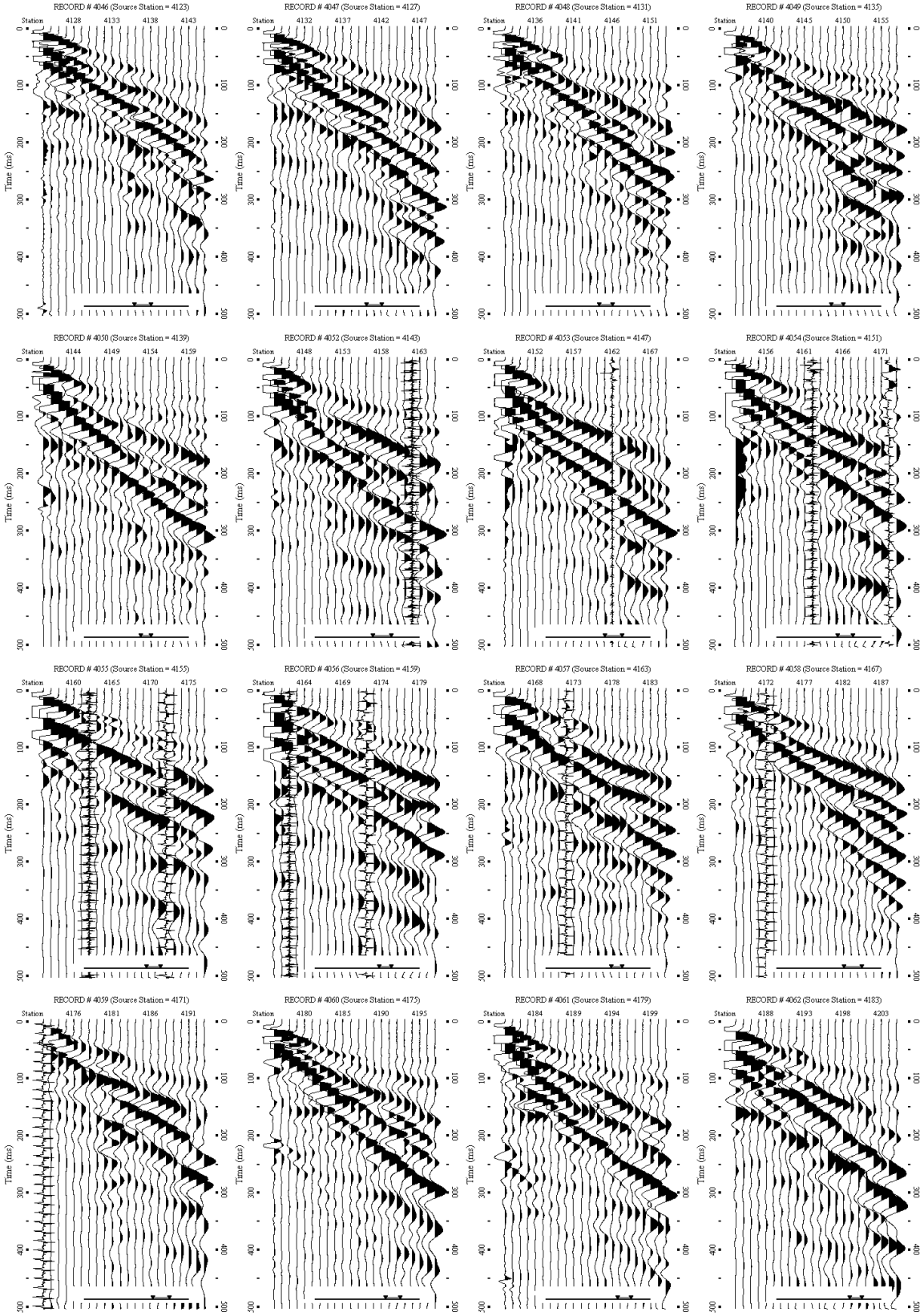

## **APPENDIX II** (continued)

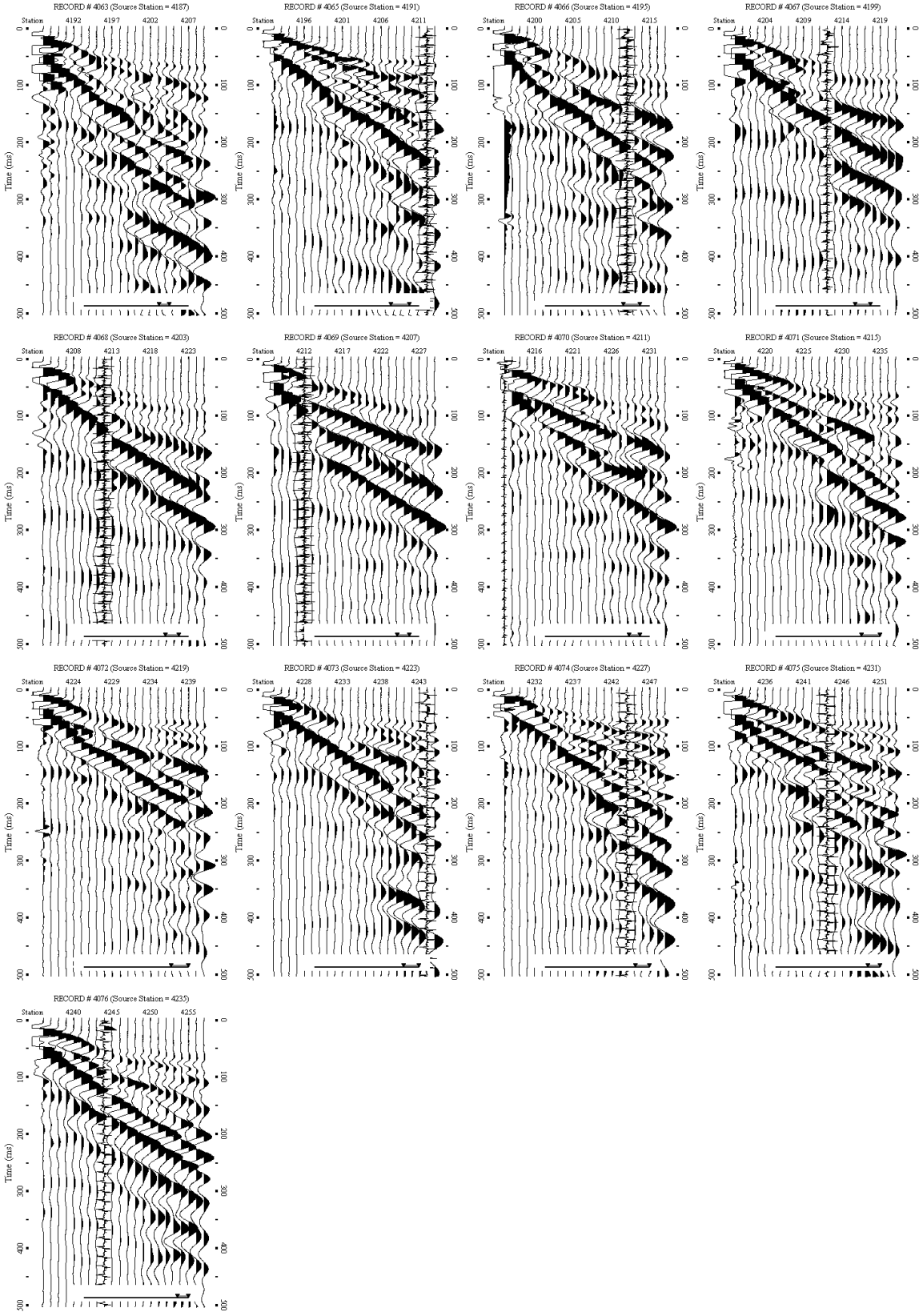

# APPENDIX III

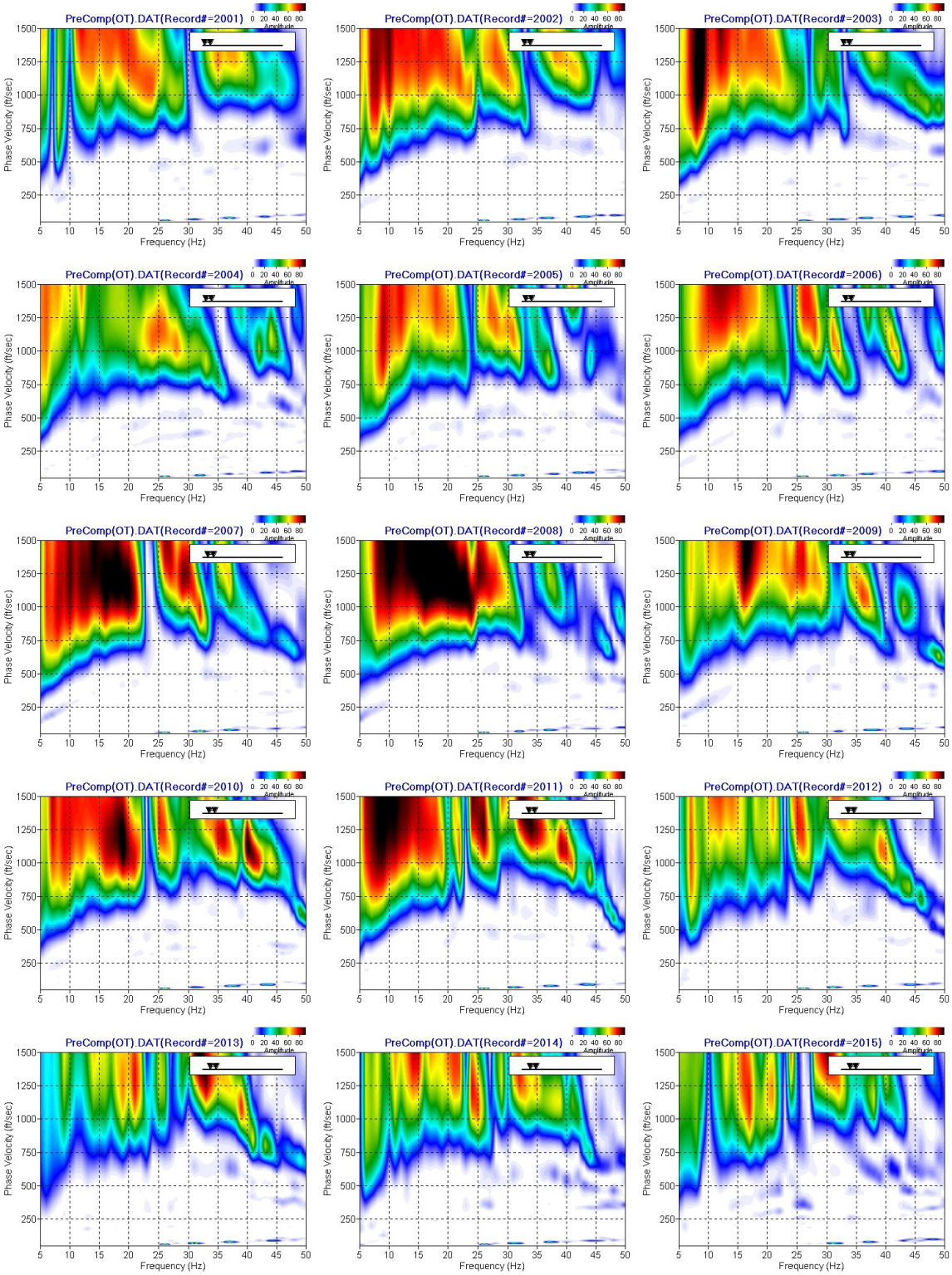

# **APPENDIX III** (continued)

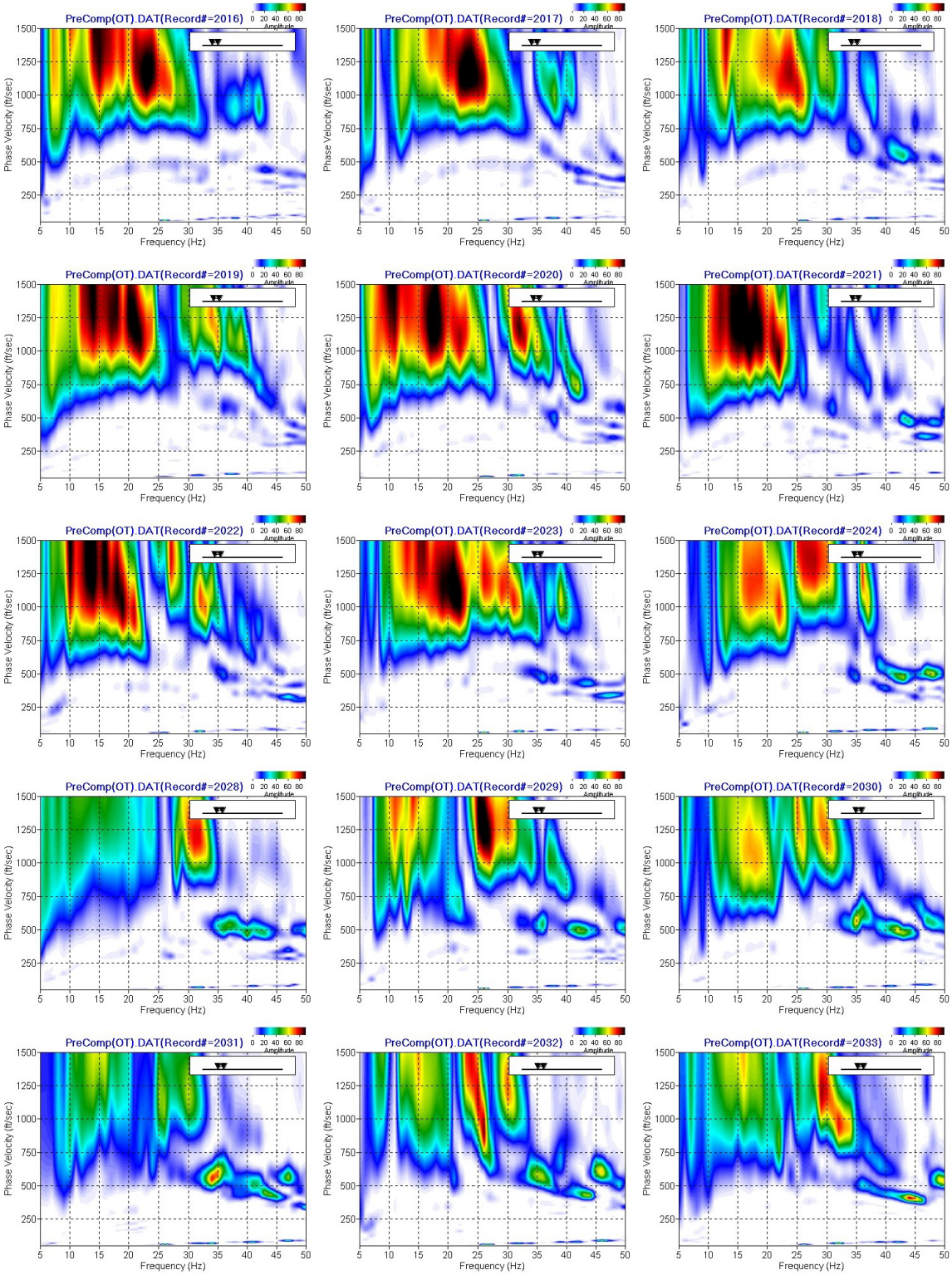

# **APPENDIX III** (continued)

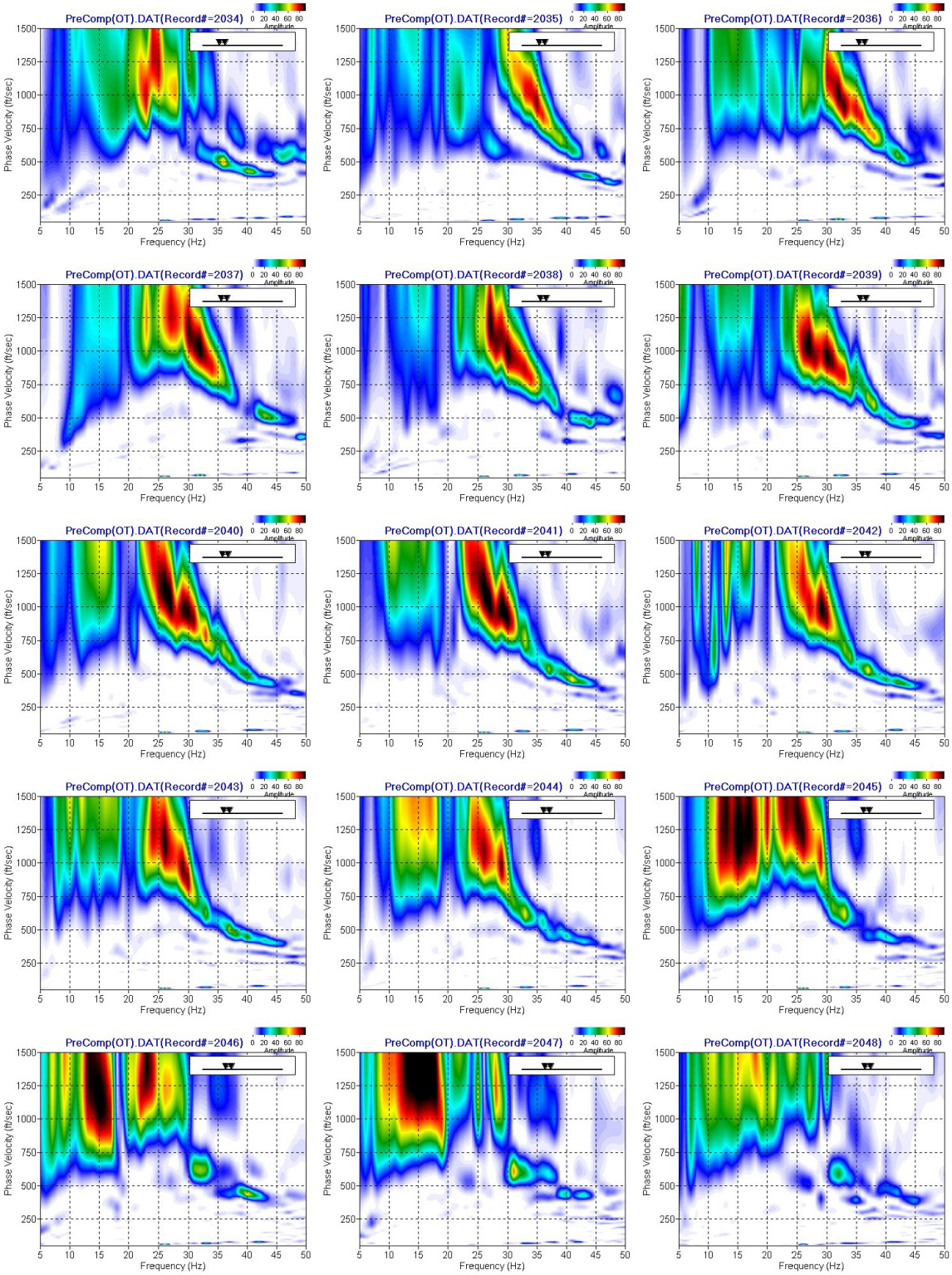

## **APPENDIX III** (continued)

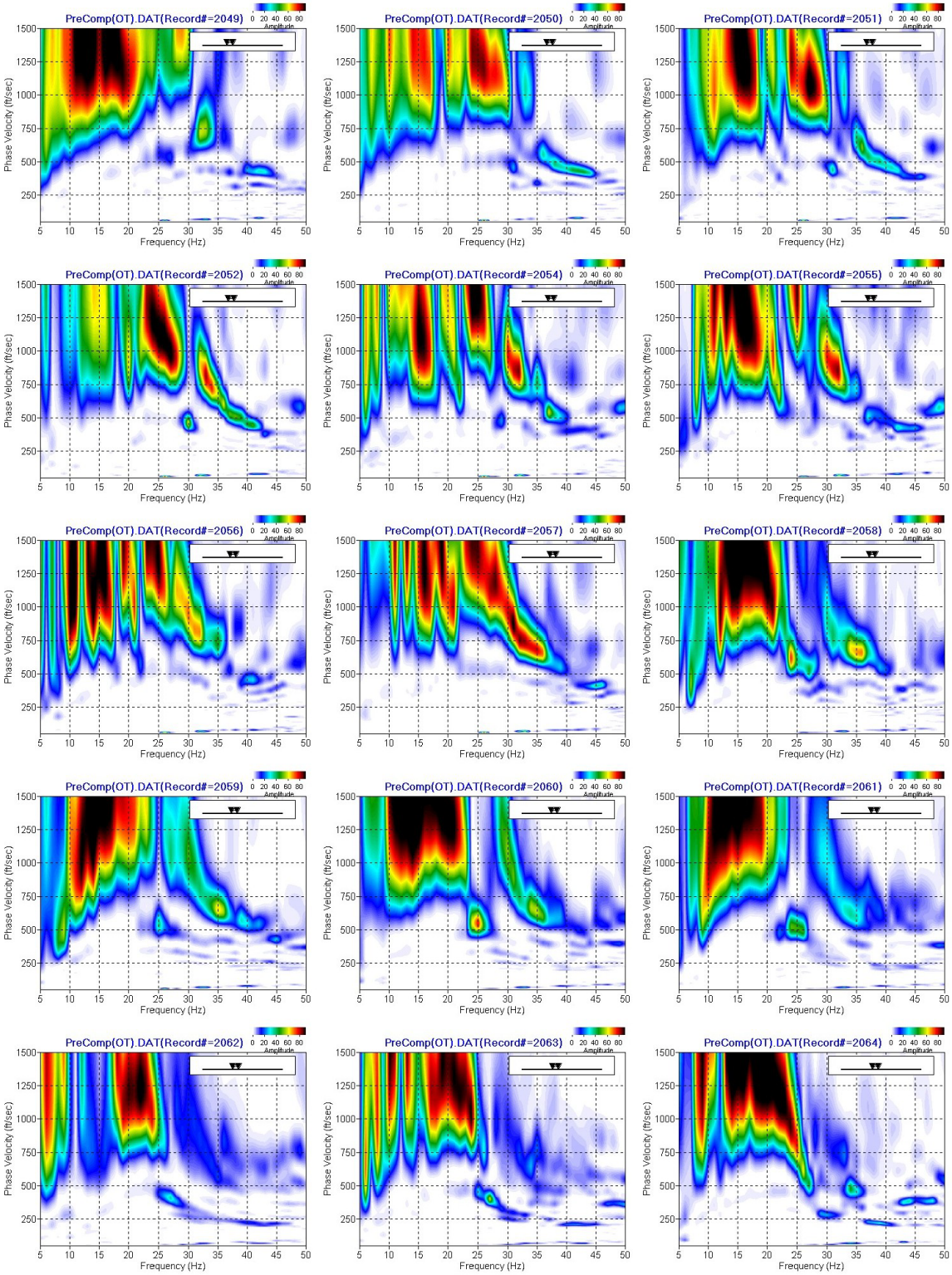

# **APPENDIX III** (continued)

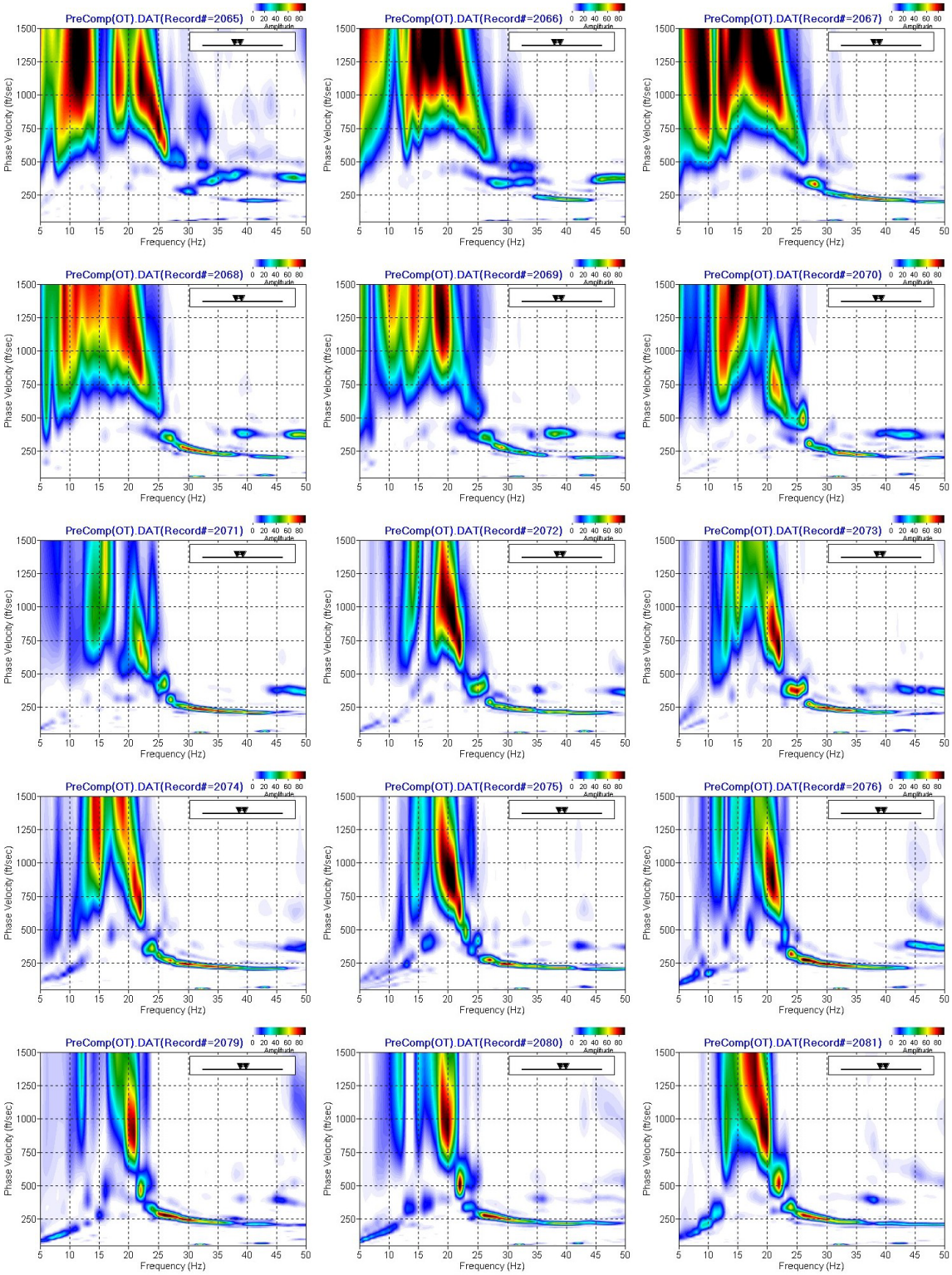

# **APPENDIX III** (continued)

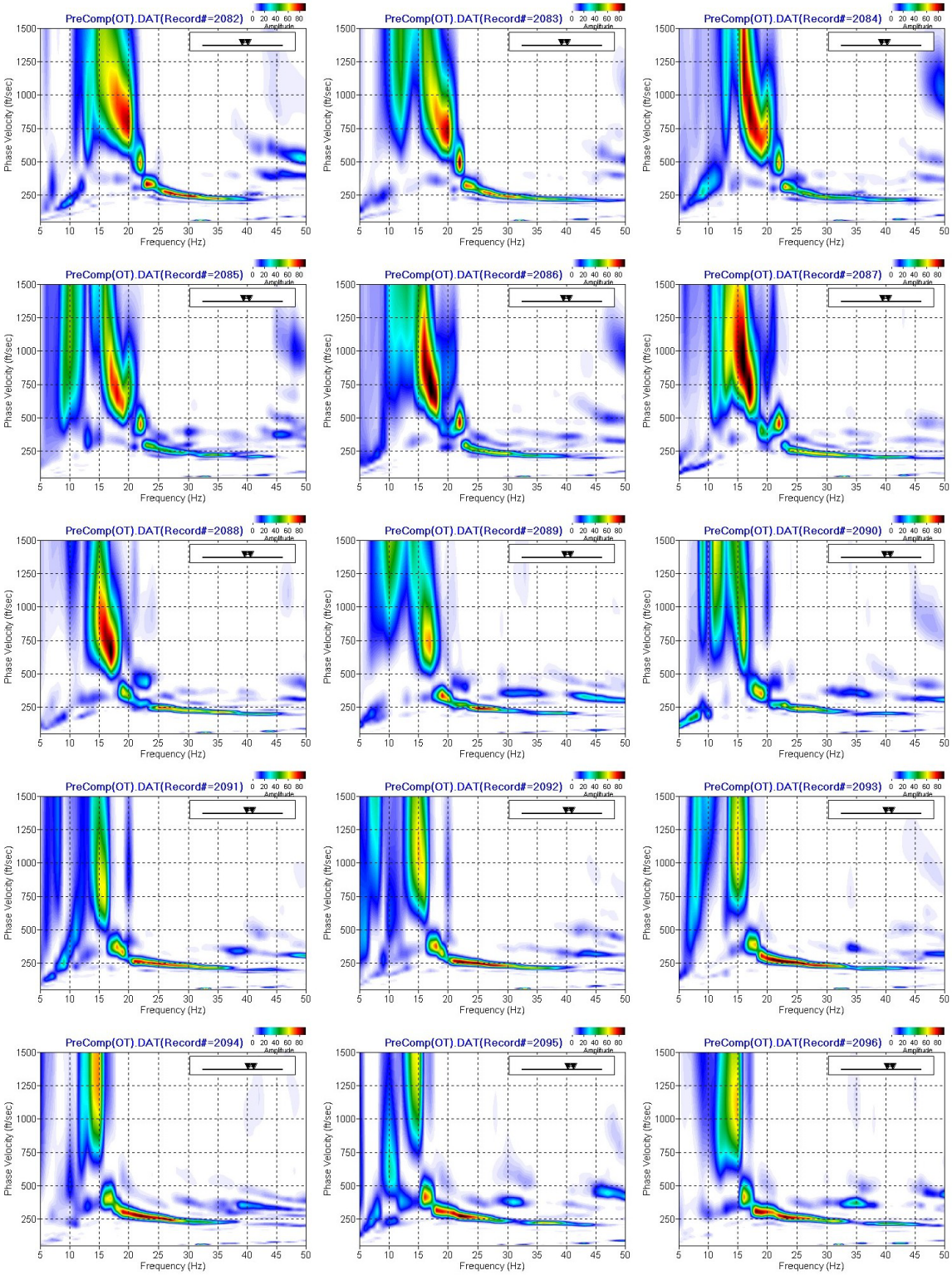

# **APPENDIX III** (continued)

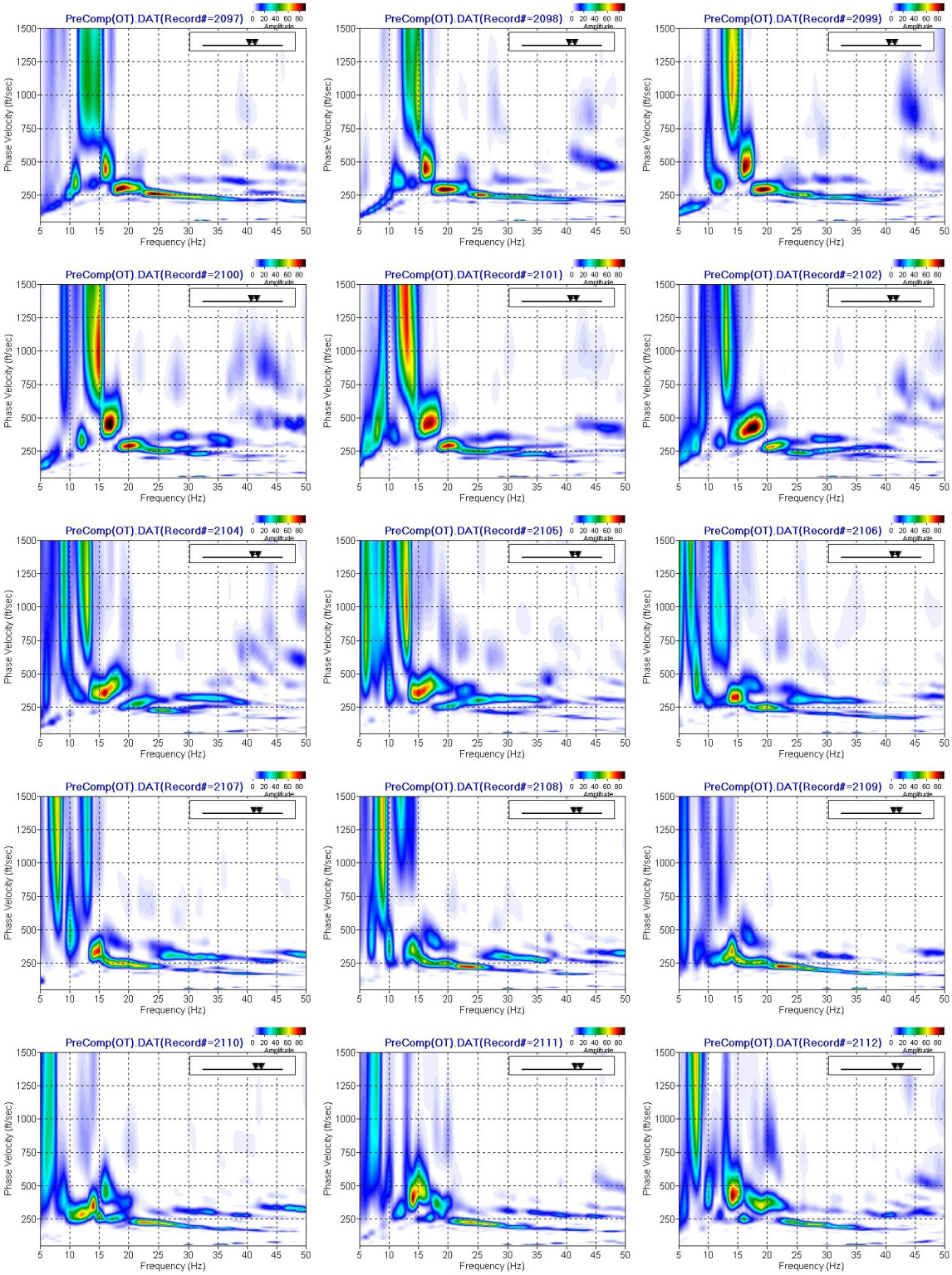

# **APPENDIX III** (continued)

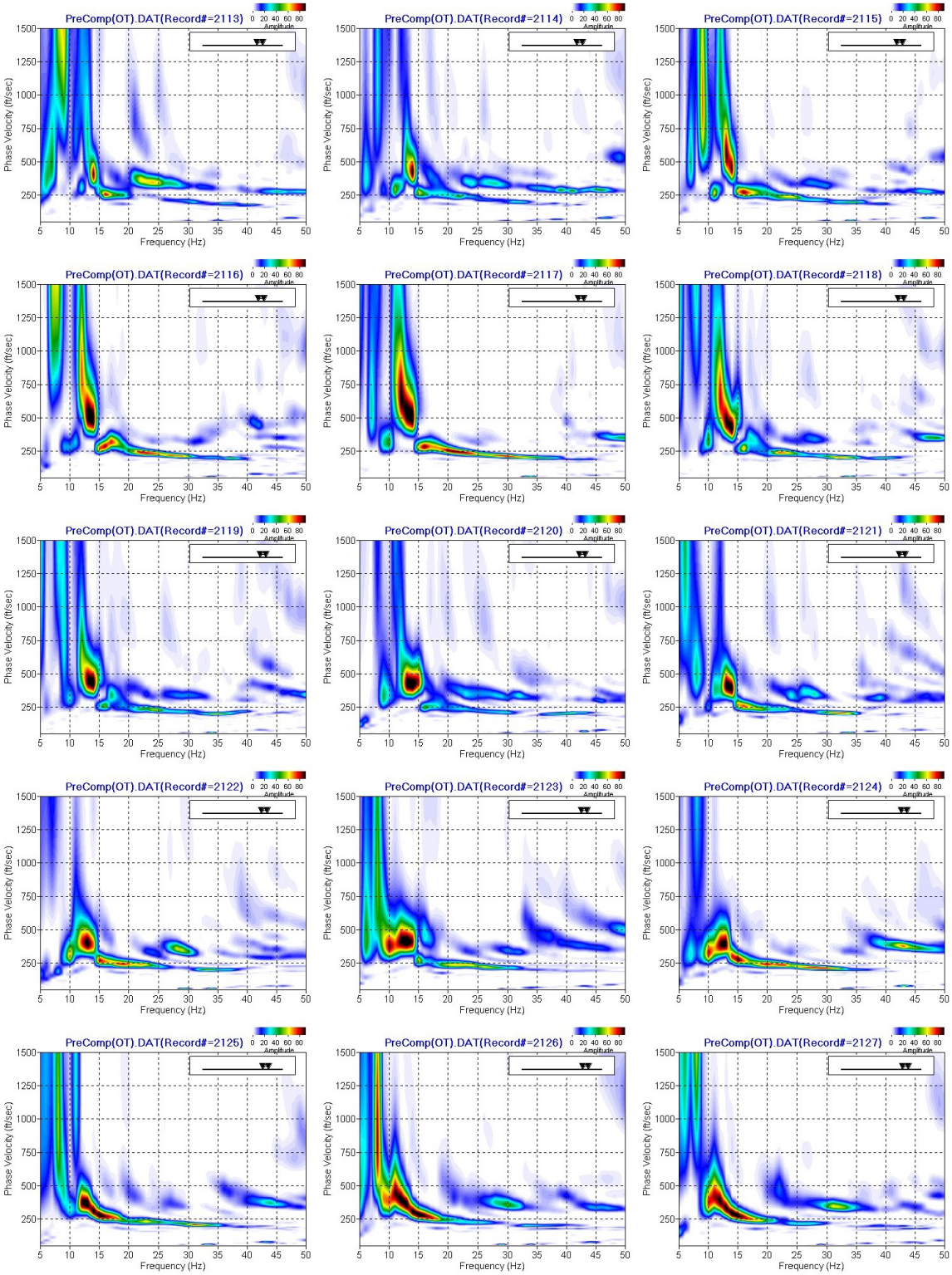

# **APPENDIX III** (continued)

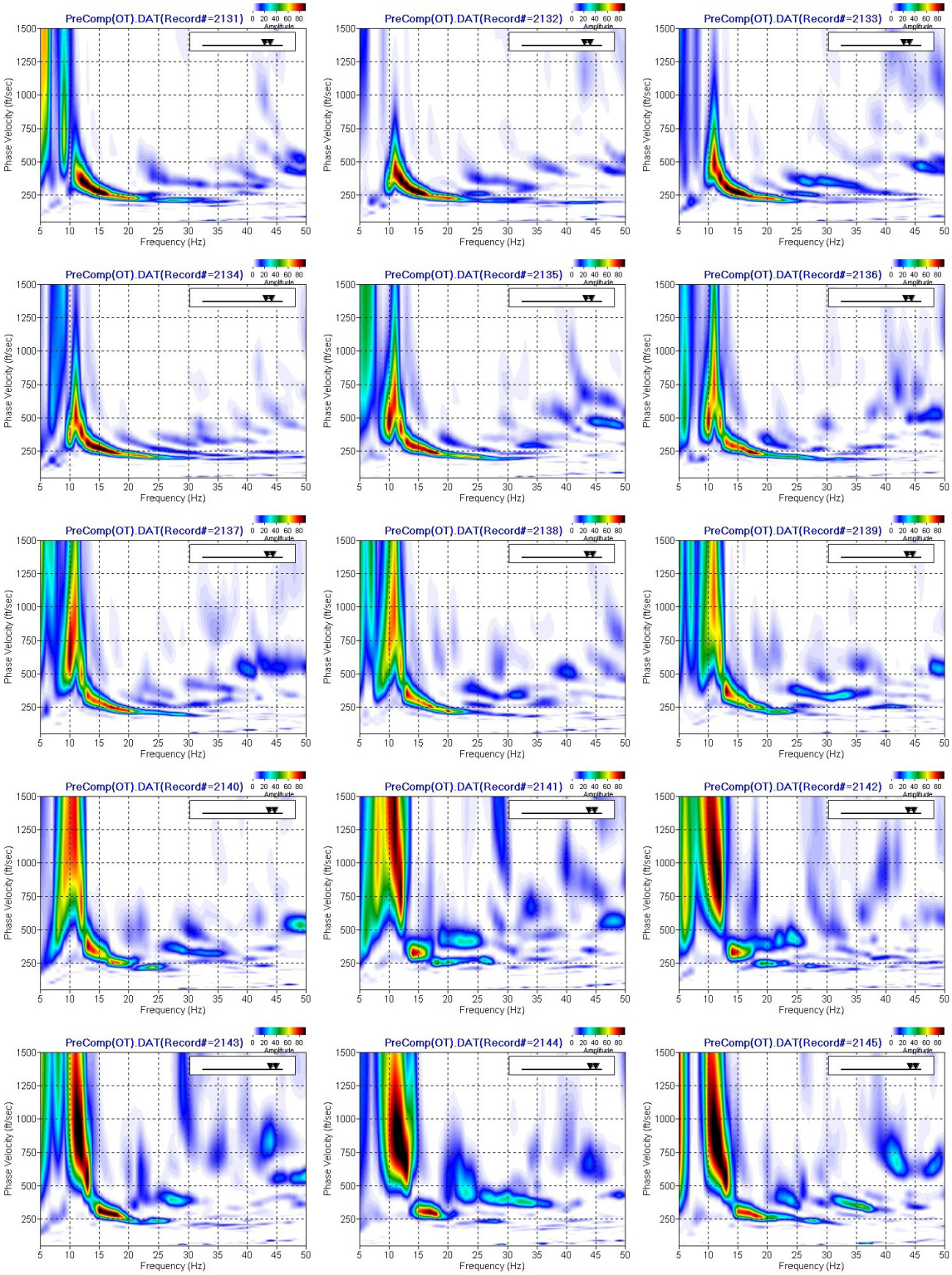

# **APPENDIX III** (continued)

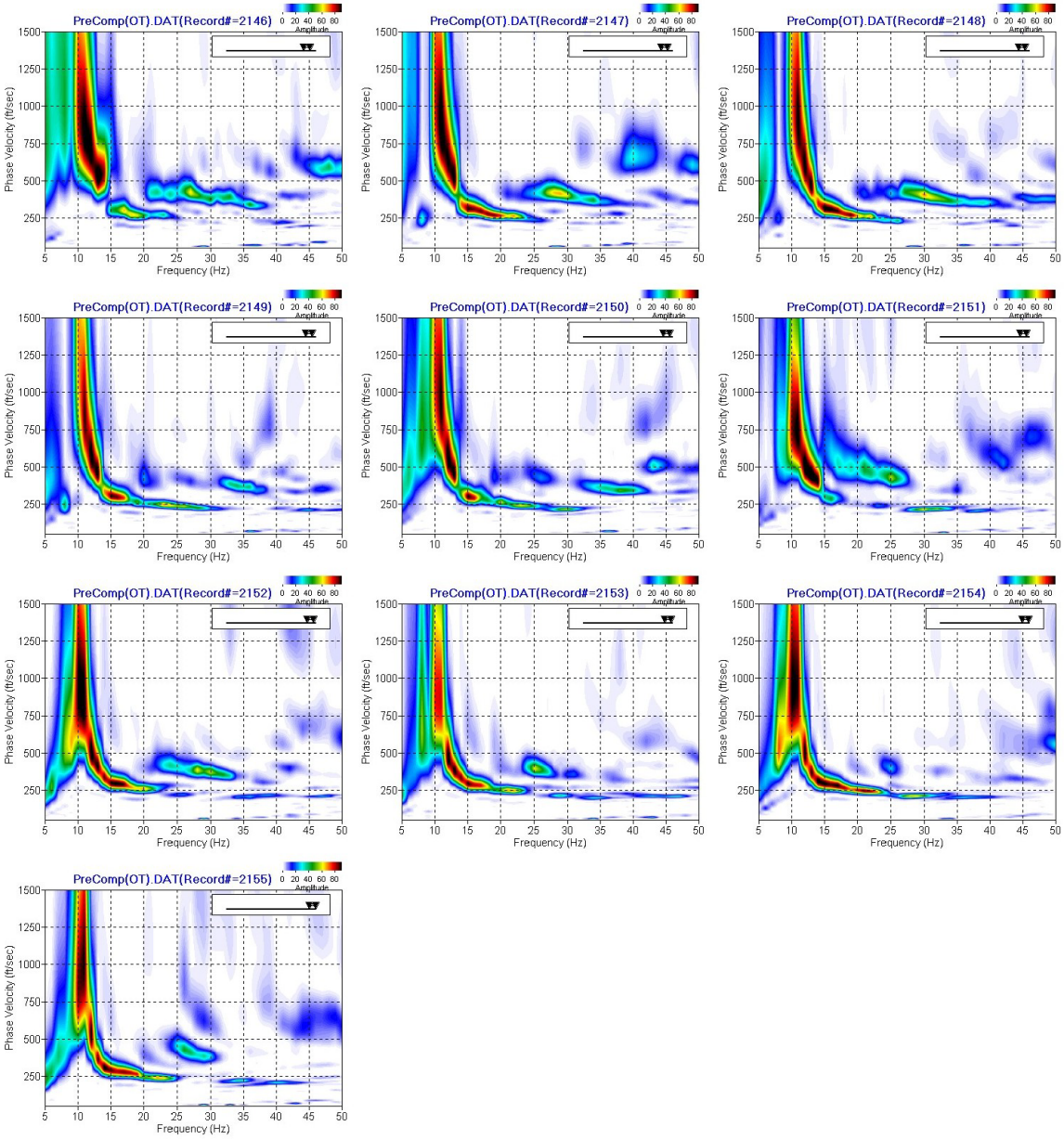

# APPENDIX IV

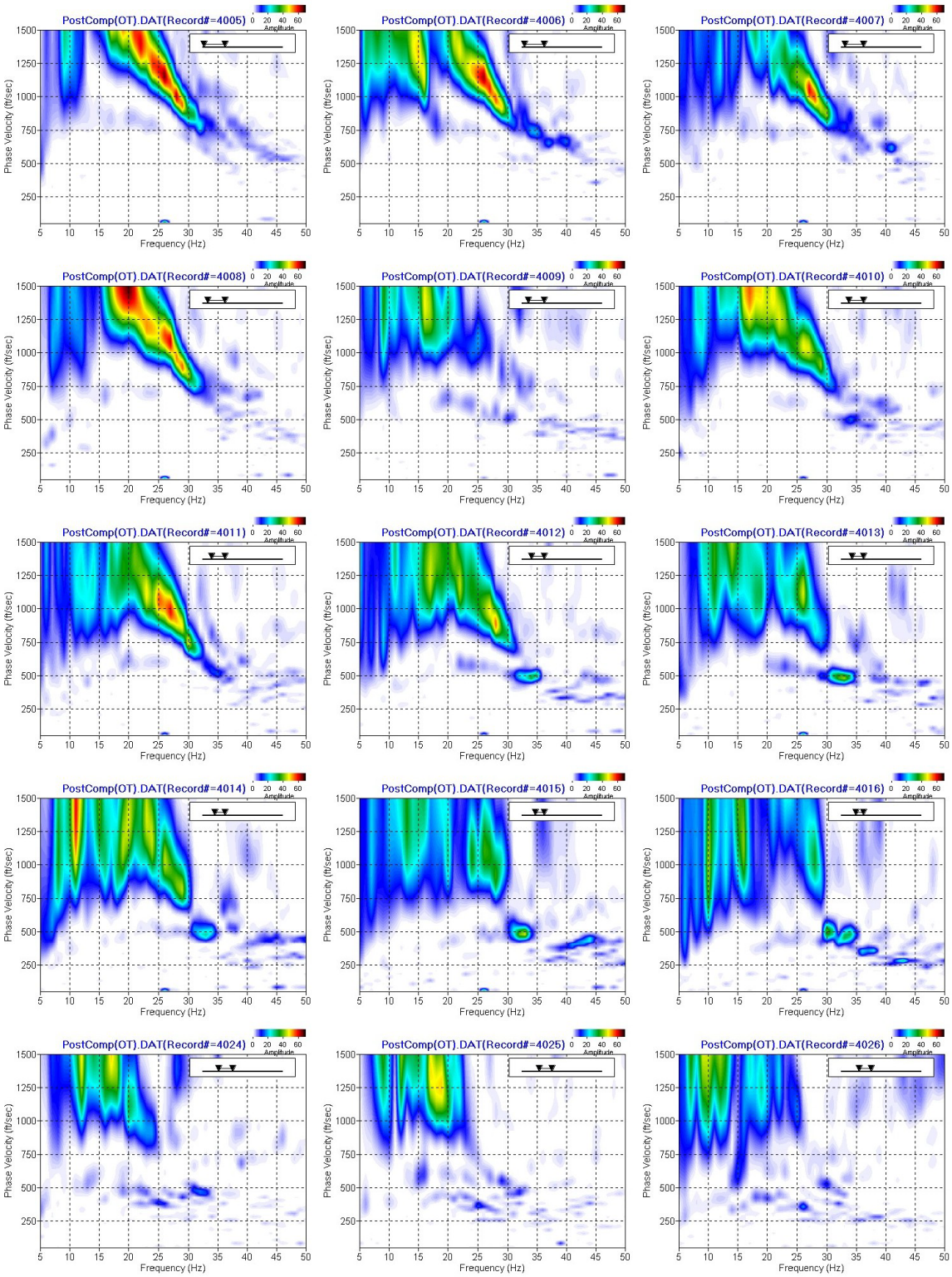
PostComp(OT).DAT(Record#=4005)
PostComp(OT).DAT(Record#=4006)
PostComp(OT).DAT(Record#=4007)
PostComp(OT).DAT(Record#=4008)
PostComp(OT).DAT(Record#=4009)
PostComp(OT).DAT(Record#=4010)
PostComp(OT).DAT(Record#=4011)
PostComp(OT).DAT(Record#=4012)
PostComp(OT).DAT(Record#=4013)
PostComp(OT).DAT(Record#=4014)
PostComp(OT).DAT(Record#=4015)
PostComp(OT).DAT(Record#=4016)
PostComp(OT).DAT(Record#=4024)
PostComp(OT).DAT(Record#=4025)
PostComp(OT).DAT(Record#=4026)
Amplitude
Phase Velocity (ft/sec)
Frequency (Hz)

# **APPENDIX IV** (continued)

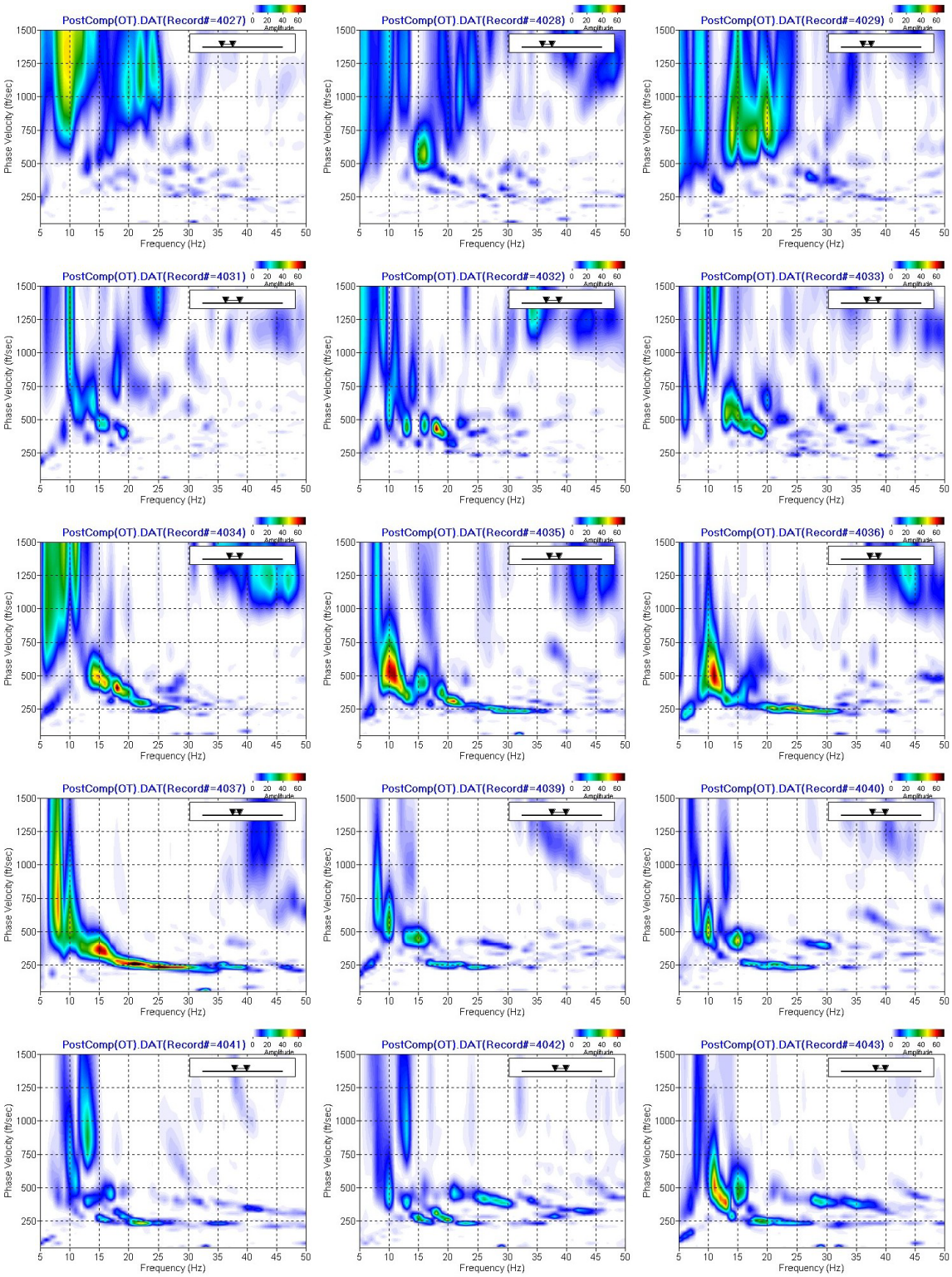

## **APPENDIX IV** (continued)

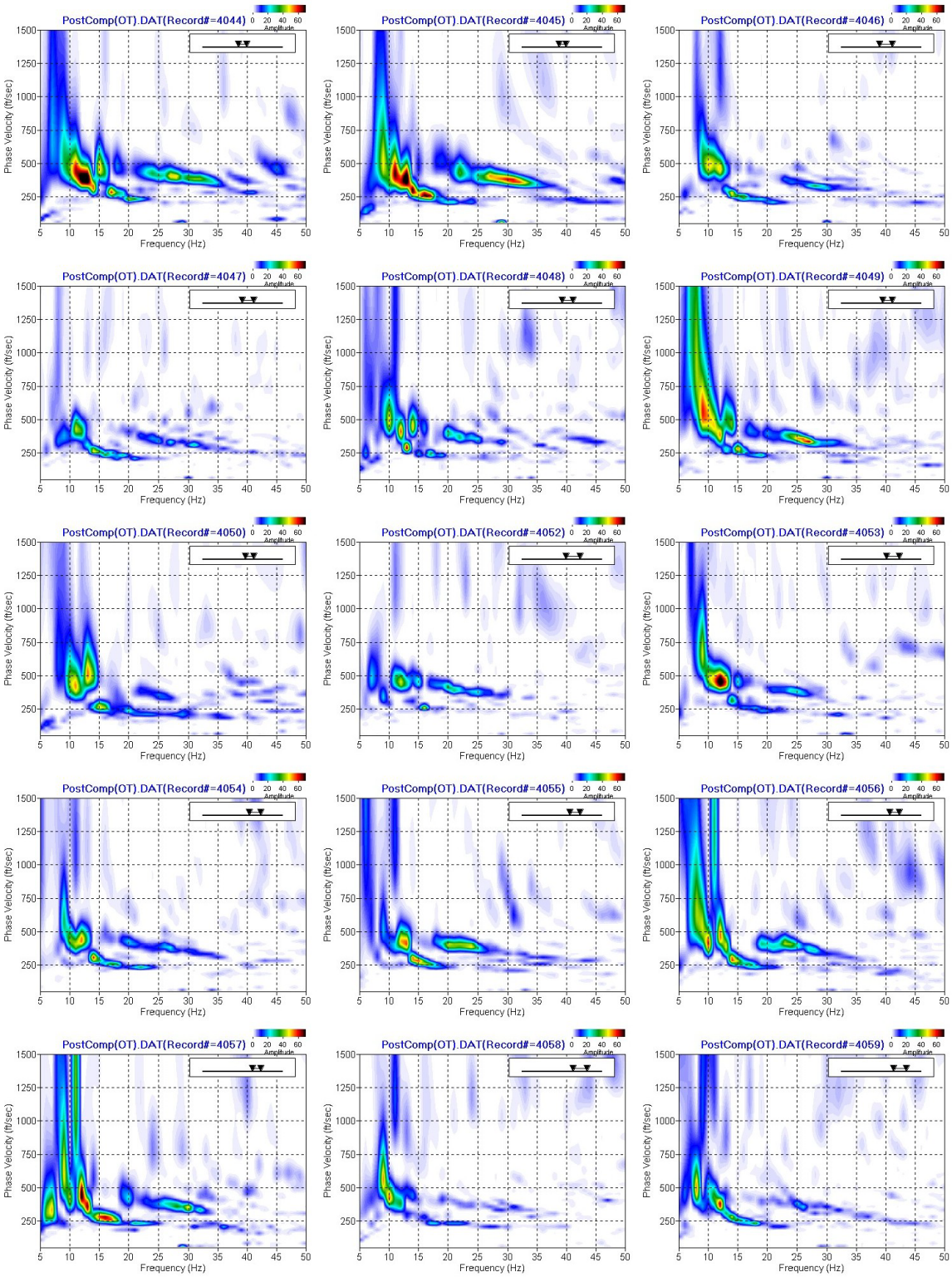

# **APPENDIX IV** (continued)

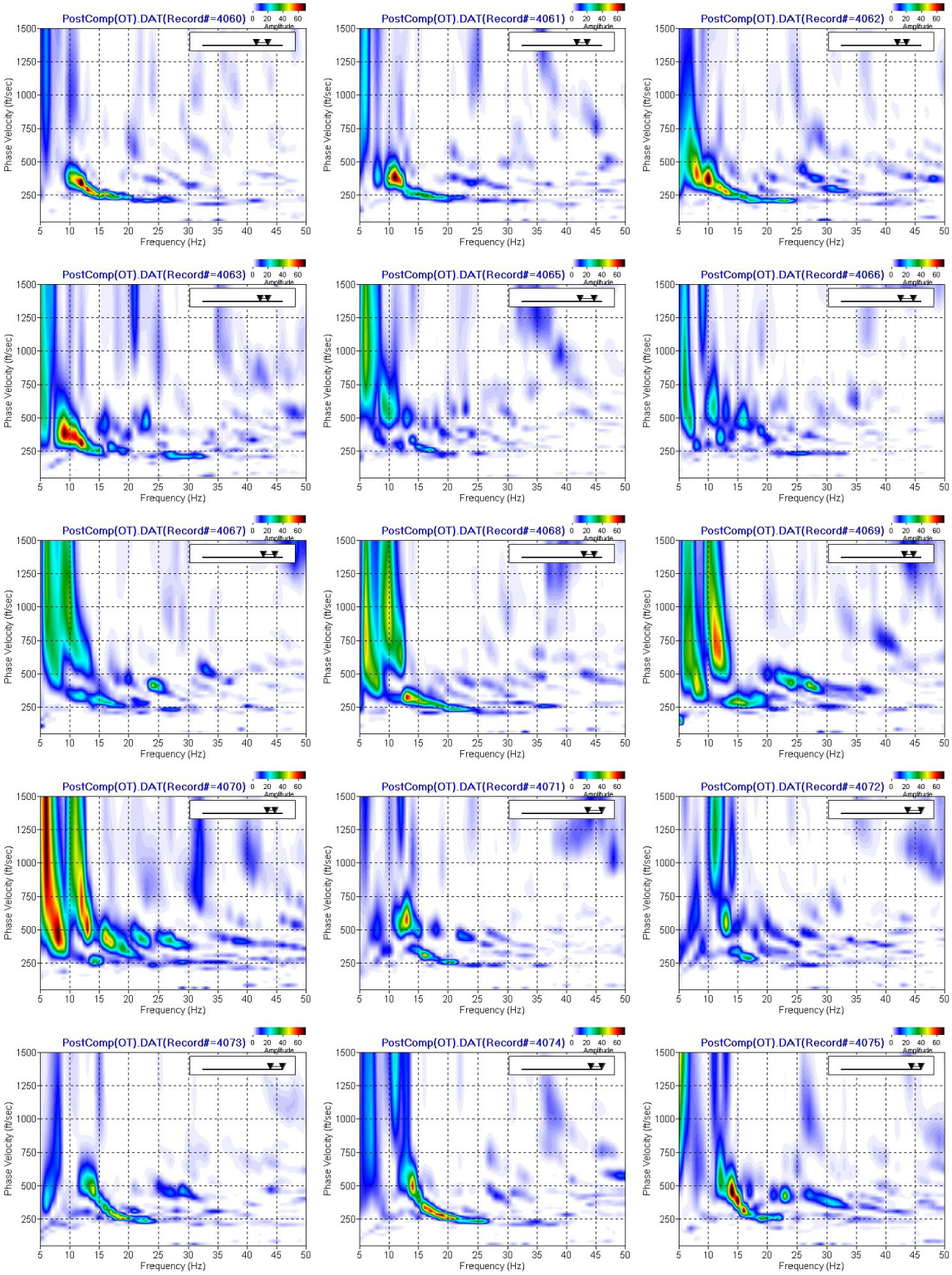

## **APPENDIX IV** (continued)